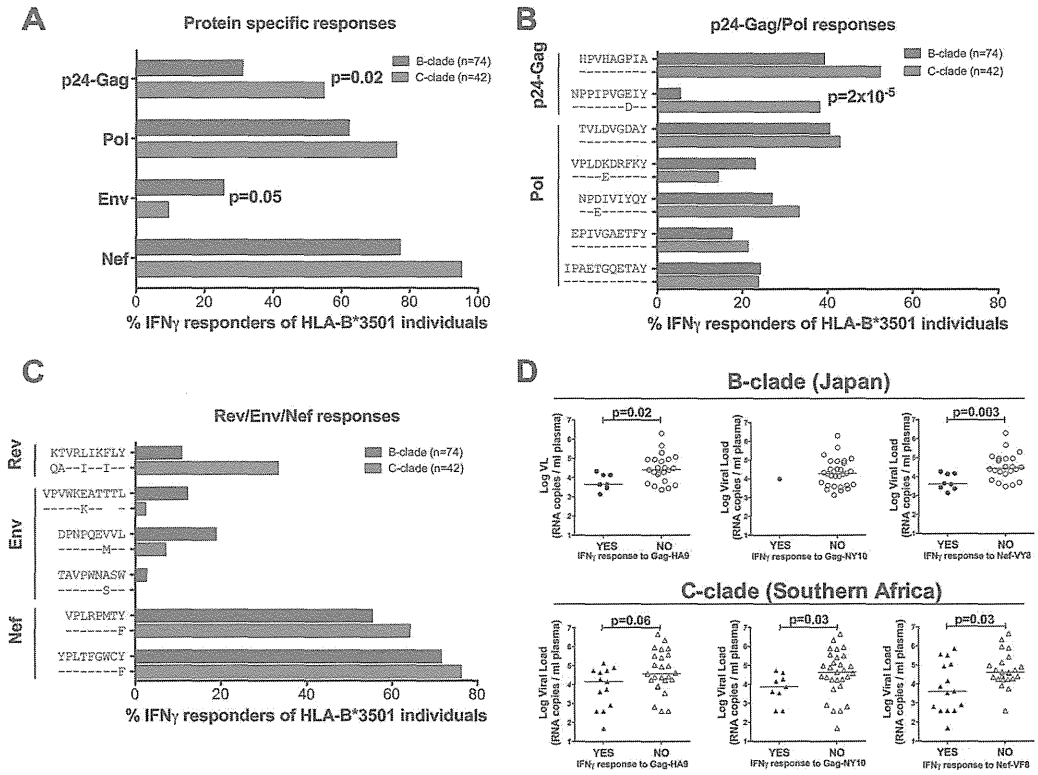

FIG 4 Percentage of HLA-B*3501-positive subjects making IFN-γ ELISpot responses to 13 HLA-B*3501-restricted epitopes in B- and C-clade infection and the impact on viral load to HA9 Gag, NY10 Gag and VY/VF8 Nef responses controlled by HLA-B*3501 matched nonresponding individuals. (A) Responses expressed as protein specific were obtained by pooling the percentage of adult HLA-B*3501-positive subjects with B-clade infection (Kumamoto, Japan) making IFN-γ ELISpot responses to individual HLA-B*3501-restricted optimal peptides (n = 30 subjects) pooled with another B-clade cohort (23, 44) screened against 18-mer overlapping peptides containing the optimal epitopes (n = 44 subjects) (blue) (total of 74 B-clade-infected subjects) and compared to adult subjects with C-clade infection (southern African subjects) tested against C-clade consensus overlapping peptides containing the corresponding optimal peptides (n = 42 subjects) (red). (B) Responses as in panel A but shown for individual epitopes within Gag and Pol proteins. (C) Responses as in panel A but shown for individual epitopes within Rev, Env, and Nef proteins. (D) Comparison of viral load between responders and nonresponders for B-clade-infected Japanese subjects (n = 30), based on responses to optimal peptides, HA9 Gag (left), NY10 Gag (middle), and VY/VF8-Nef (right) (top panels) and C-clade southern African subjects based on responses to OLPs containing the corresponding optimal peptides (bottom panels). In each case, a positive ELISpot response is defined as >100 SFC/10^6 PBMCs; P values are by Fisher's exact test (A, B, and C) (and for B and C are shown only when significant after correction for multiple comparisons) or by Mann-Whitney U test (D).

Gag NY10 is the single epitope differentially targeted by HLA-B*3501 subjects with B- and C-clade infection. Reactivity to the panel of HLA-B*3501-restricted epitopes defined was determined in HLA-B*3501-positive subjects with B-clade infection (n = 74) and in subjects with C-clade infection (n = 42) using ELISpot assays (Fig. 4). Overall, p24 Gag-specific epitopes were targeted significantly more frequently by the C-clade-infected B*3501-positive study subjects (55% versus 31%; P = 0.02 by Fisher's exact test), whereas Env-specific epitopes were targeted more frequently by B-clade-infected B*3501-positive study subjects (10% versus 26%; P = 0.05 by Fisher's exact test) (Fig. 4A). At the individual epitope level, the single statistically significant clade-specific difference was in the response to the Gag NY10 epitope (Gag positions 253 to 262; $P = 2 \times 10^{-5}$). A response to this epitope was seen in only 5% of B-clade-infected subjects, versus 38% of C-clade-infected subjects. Although the Rev epitope KY10 (Rev positions 14 to 23) was also predominantly targeted in C-clade infection, this difference in recognition in B- and C clade-infected HLA-B*3501-positive subjects did not reach statistical significance after correction for multiple comparisons.

Both p24 Gag responses and one Nef response are consistently associated with lower viral load in subjects with HLA-B*3501. Having determined which HLA-B*3501-restricted epitopes are targeted in B- and C-clade-infected subjects with HLA-B*3501, we next investigated which of these responses appear to be most effective in bringing about a low viral set point. Two responses were consistent in being associated with a lower set point in the responders compared to the nonresponders in both B- and C-clade cohorts, Gag HA9 and Nef VY8 (Fig. 4D). These two epitopes are targeted equally well in B- and C-clade infection, and therefore these responses do not help to explain why HLA-B*3501 is associated with lower viral set points in C-clade infection. In the case of Gag NY10, however, in B-clade infection there was only 1 responder among 31 B-clade subjects for whom viral loads were available. However, in the C-clade-infected cohort, a response toward Gag NY10 was also associated with a lowered viremia (P = 0.03 by Mann-Whitney test) (Fig. 4D), Thus, the only HLA-B*3501-restricted response associated with a lower viral set point for which there was a significant difference in epitope targeting comparing the B- and C-clade cohorts was the Gag NY10 response.

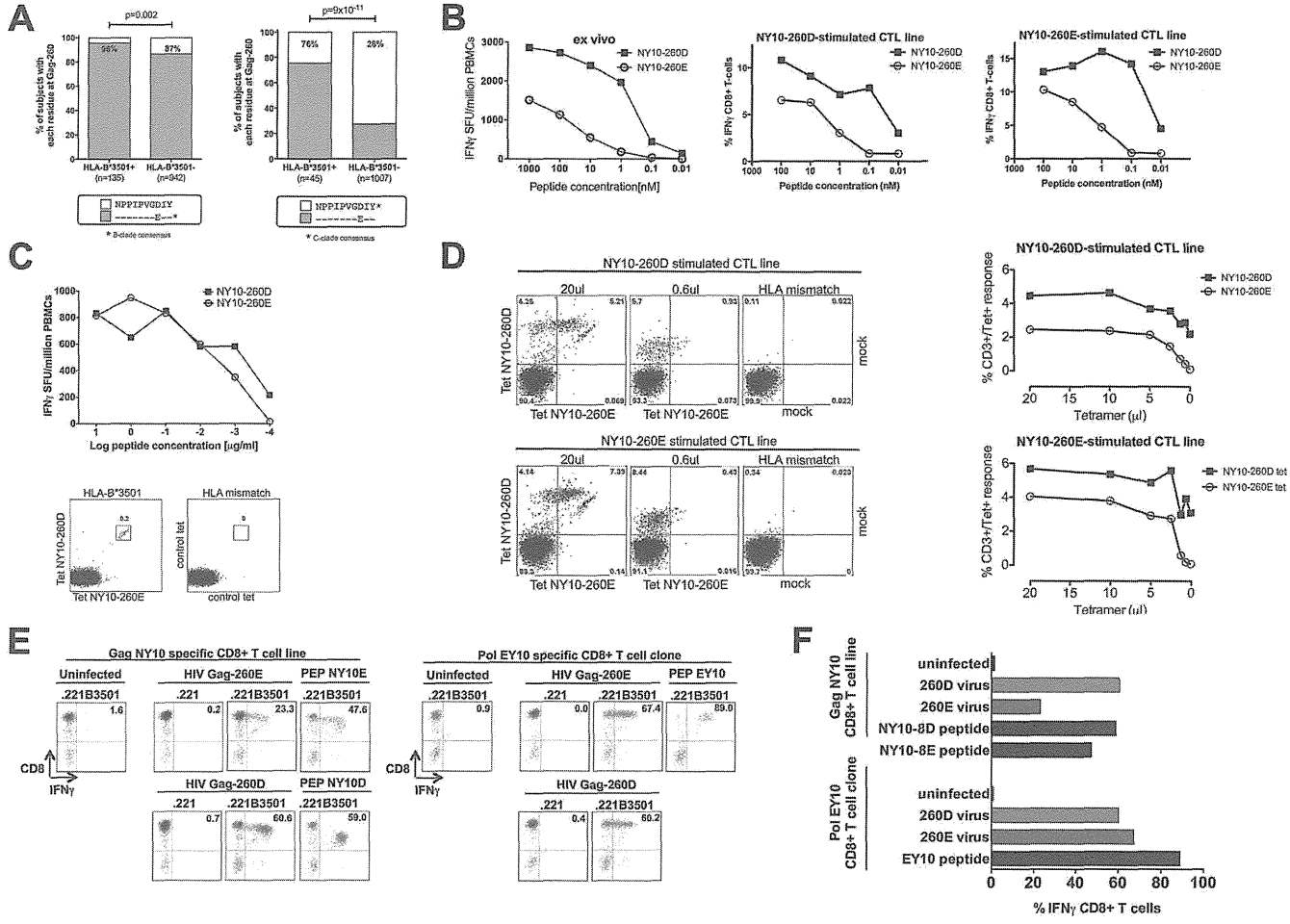

FIG 5 Selection of Gag-D260E substitution in C-clade infection and effect of this polymorphism on $CD8^+$ T-cell recognition and lack of NY10-260E specific $CD8^+$ T cells. (A) Selection of Gag-D260E polymorphism in subjects with HLA-B*3501 from an extended B-clade data set as previously published (24) (n = 1,077; total subjects with HLA-B*3501, n = 135 [12.5%]) (left) and selection of Gag-D260E polymorphism in subjects with HLA-B*3501 from an extended southern African data set (Durban, n = 695; Botswana, n = 298; Thames Valley Africans, n = 59; total subjects with HLA-B*3501, n = 45 [4.3%]) (right). (B) IFN-γ *ex vivo* ELISpot responses made by an HLA-B*3501-positive Japanese subject with chronic B-clade infection (subject KI705, HLA-A*2402, -A*2601, -B*3501, -B*5201, -Cw*0303, -Cw*1202) to optimal epitope NY10 (NPPIPVGDIY) and an escape variant containing the D260E substitution (NPPIPVGEIY) and IFN-γ intracellular cytokine staining of $CD8^+$ T cells *in vitro* expanded and tested against titrated amounts of NY10-260E and NY10-260D peptides. One experiments was performed. (C) IFN-γ *ex vivo* ELISpot responses made by an HLA-B*3501-positive subject with chronic B-clade infection (subject OX035, HLA-A*0201, -A*1101, -B*1801, -B*3501, -Cw*0401, -Cw*0501) to optimal epitope NY10-260D and an escape variant containing the D260E substitution NY10-260E and dual NY10-260E and NY10-260D HLA-B*3501 tetramer staining of *ex vivo* PBMCs controlled by HLA-B*4201 mismatch tetramer. Results from one representative of two independent experiments are shown. (D) *In vitro*-expanded PBMCs from subject OX035 using NY10-260D (top) and NY10-260E (bottom) peptides and stained with titrated amounts of dual HLA-B*3501 tetramers (260D/260E) gated on $CD8^+$ T cells (dot plots) and expressed as $CD3^+/Tet^+$ positive cells for all tetramer titrations (right) controlled by HLA-B*4201 mismatch tetramers. P values are by Fisher's exact test. One experiments was performed. (E and F) HLA-negative and HLA-B*3501-expressing target cells were infected with either Gag-260E or Gag-260D virus and tested for epitope recognition by specific $CD8^+$ T cells determined by IFN-γ production after coculture and shown for Gag-NY10 epitope processing (left) or the control Pol-EY10 epitope (right) by fluorescence-activated cell sorter (FACS) plots (E) and shown as horizontal bar graphs (F). Peptide-pulsed target cells (PEP) were included as a positive control for optimal epitope presentation.

Lack of immunogenicity of NY10-260E indicated by strong selection of the Gag-D260E polymorphism in B- and C-clade infection and lack of NY10-260E-specific $CD8^+$ T-cell responses. We next addressed the question of why the B-clade version of Gag NY10, which differs from the C-clade version only at position 8 in the epitope, in the replacement of Asp by Glu (Gag-D260E), appears to be nonimmunogenic, whereas the C-clade version is highly immunogenic. Although 38% of HLA-B*3501-positive subjects with chronic C-clade infection show detectable responses to NY10-260D, analysis of *gag* sequences in the cohort indicates that exactly twice that figure, 76%, of HLA-B*3501-positive subjects carry the Gag-D260E mutation, compared to 28% of the HLA-B*3501-negative study subjects (Fig. 5A) ($P = 9 \times 10^{-11}$). We confirmed that, in every case tested, the NY10-D260E variant is substantially less well recognized than the C-clade wild-type NY10-260D (Fig. 5B) and that NY10-D260E is therefore an escape mutant. Strikingly, NY10-260E is also selected in HLA-B*3501-positive subjects with B-clade infection (Fig. 5A), in spite of the fact that close to 90% of B-clade sequences carry Gag-260E (37). These data suggest that NY10-260E is nonimmunogenic and that only the small fraction of B-clade-infected HLA-B*3501-positive subjects presented with virus expressing the Gag-260D vari-

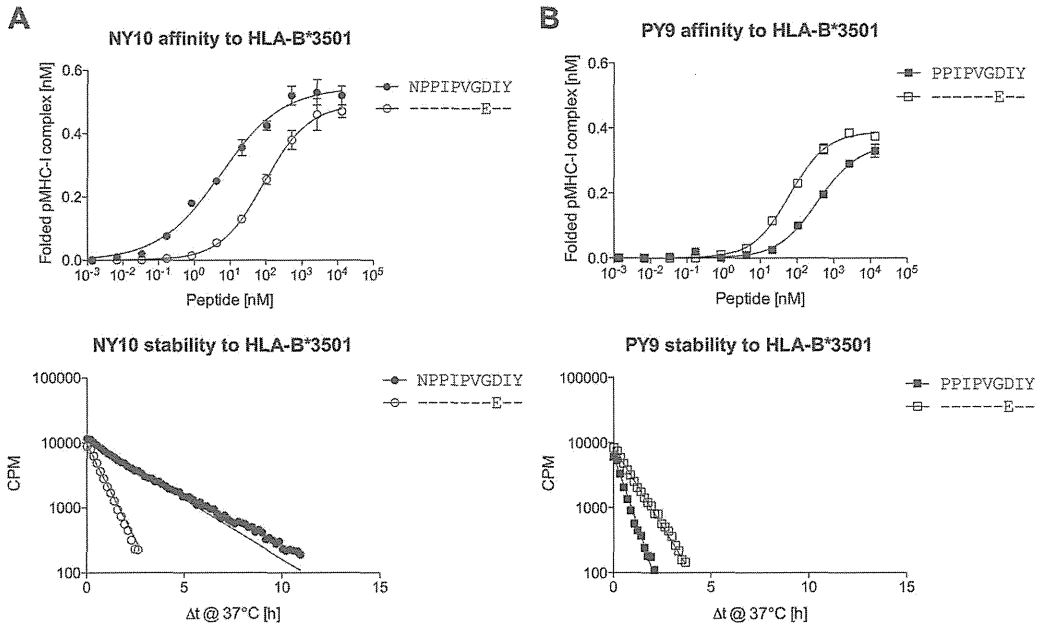

FIG 6 Binding of NY10 Gag and PY9-Gag to the HLA-B*3501 molecule. Strength of binding affinity (K_d, nM) of HLA-B*3501 was determined using the luminescent oxygen channeling immunoassay, as previously described (29) (top panels), and stability half-life ($t_{1/2}$) of binding (h) was determined using scintillation proximity assay, as previously described (30) (bottom panels), for NY10 (A) and PY9 (B). Results from one representative of four independent experiments are shown.

ant can make an NY10-260D-specific response, from which the viral escape mutant D260E is selected.

To test this hypothesis, i.e., that NY10 responses in B-clade-infected subjects are either cross-reactive between the two NY10-260D and NY10-260E variants or specific to the NY10-260D form but are never specific for the NY10-260E variant, we generated HLA-B*3501-NY10-260D and HLA-B*3501-NY10-260E tetramers with which to stain NY10-specific $CD8^+$ T cells. Staining of PBMCs and antigen-specific cell lines with these two HLA-B*3501-NY10 tetramers was consistent with the hypothesis (Fig. 5C and D). *In vitro* expansion of NY10-specific $CD8^+$ T cells in the rare B-clade-infected persons showing a response to this epitope showed, irrespective of which variant had been used to stimulate PBMCs, preferential recognition of the NY10-260D (C-clade version) of the epitope (Fig. 5B). Where there is apparent cross-reaction of NY10-260D-specific $CD8^+$ T cells to the NY10-260E variant (Fig. 5C), following *in vitro* expansion of these cells using either the NY10-260D or the NY10-260E peptide, preferential recognition of the NY10-260D epitope consistently emerges. Dual NY10-260D and NY10-260E tetramer staining confirms that only cross-reactive or NY10-260D-specific $CD8^+$ T cells exist, with no detection of NY10-260E-specific $CD8^+$ T cells (Fig. 5D). To test whether the 260E escape version has a reduced recognition compared to the 260D version using intracellular processed epitopes, rather than peptide-pulsed cells, we infected HLA-B*3501-positive or HLA class I-negative cells with HIV containing either the 260D or the 260E virus and determined the level of NY10 epitope recognition by assaying the activation of an NY10-specific $CD8^+$ T-cell line after coculture with cells infected for 6 days (Fig. 5E and F). We detected almost 3-fold-higher activation after infection with the 260D virus compared to the 260E virus ($CD8^+$/IFN-γ^+, 60.6% versus 23.3%) but equal activation of the control Pol EY10-specific $CD8^+$ T-cell clone. Thus, infection with the 260E virus results in a markedly reduced recognition of the nonimmunogenic NY10-260E compared to the immunogenic NY10-260D epitope processed from the 260D virus.

NY10-260E nonimmunogenicity results from lack of HLA-B*3501–peptide binding affinity and stability. Given that the peptide-binding motif for HLA-B*3501 does not show any preference for particular residues at position 8 (P8) in the epitope, our initial hypothesis was that nonimmunogenicity of the NY10-260E variant might be related to the low TcR repertoire available for HLA-B*3501-restricted T-cell responses, as proposed by Kosmrlj et al. (41). However, to determine whether that NY10-260E nonimmunogenicity might be more readily explained as a result of weak HLA-B*3501 binding affinity and/or stability, we first performed these MHC binding studies. We found that the immunogenic, NY10-260D (C-clade) version of the peptide had a >10-fold-greater binding affinity to the HLA-B*3501 molecule than the NY10-260E (B-clade) variant and was more than three times more stable in complex with the HLA-B*3501 molecule than the NY10-260E version (half-life, 1.6 h versus 0.5 h) (Fig. 6A). Previous studies suggest that, with rare exceptions, a peptide-MHC stability half-life of >1 h is required for peptides to be immunogenic (31). The low peptide-MHC binding stability of the NY10-260E variant (half life, 0.5 h) would therefore explain the lack of NY10-specific responses observed for the B-clade cohorts studied here. This is also consistent with reduced recognition of the NY10-260E versus the NY10-260D version of the epitope shown in Fig. 5.

It is noteworthy that had PY9 as opposed to NY10 been the optimal epitope in this case, it would not have been able to explain lack of immunogenicity of the B-clade variant in this way. Both B- and C-clade versions of PY9 had low peptide-binding affinities to HLA-B*3501, in particular the Gag-260D (C-clade) version (K_d = 76 and 407 nM for PY9-260E and PY9-260D, respectively), and very low peptide-B*3501 binding stabilities, again lower for the

Gag-260D C-clade version of PY9 (half-life of 0.62 h and 0.34 h for PY9-260E and PY9-260D, respectively).

Together these data suggest that the observed differential HLA-B*3501 association with HIV disease progression in B- and C-clade infection may hinge on a single Gag epitope, NY10, and that the lack of immunogenicity of this epitope in B-clade infection rests on the presence of Glu at Gag-260 in the consensus B-clade sequence, in contrast to Asp at Gag-260 in the consensus C-clade sequence.

DISCUSSION

The data presented here demonstrate that subjects with HLA-B*3501 control HIV-1 more effectively in C-clade than in B-clade infection. This difference was associated with greater targeting of p24 Gag epitopes and less frequent targeting of Env epitopes overall. However, the single epitope significantly targeted differentially was the Gag NY10 epitope, targeted by 38% of HLA-B*3501-positive subjects with chronic C-clade infection and only 5% of HLA-B*3501-positive subjects with chronic B-clade infection. The reason for this difference is the replacement of Asp by Glu at Gag-260, position 8 within the NY10 epitope: in C-clade infection, ~75% of sequences carry Asp at Gag-260, whereas in B-clade infection, ~90% of sequences carry Glu at Gag-260. NY10-260E is nonimmunogenic and insufficiently recognized from infected cells (<25% $CD8^+$ T-cell activation) because this variant fails to bind sufficiently stably to HLA-B*3501. In contrast, the NY10-260D version is recognized more efficiently (>60% $CD8^+$ T-cell activation) and binds relatively stably to HLA-B*3501 (off-rate half-life of 1.6 h, compared to 0.5 h for NY10-260E). The binding affinity of HLA-B*3501 for NY10-260D was also substantially higher than that for NY10-260E (K_d of 10 nM versus 113 nM, respectively), consistent with the difference in antigen processing of this epitope. These findings provide a plausible explanation for why NY10-260E is an escape variant in B- and C-clade infection and why only the NY10-260D variant is immunogenic.

Several hypotheses have previously been proposed to explain the rapid disease progression of HLA-B*3501-positive subjects infected with B-clade HIV, including a paucity of HLA-B*3501-restricted Gag-specific $CD8^+$ T-cell epitopes (39), failure to optimize antiviral NK activity (51, 52) and narrowness of the TcR repertoire available to counter epitope sequence variability (41). The data presented here support the "Gag hypothesis" (39), in that even the addition of a single extra Gag response appears to significantly alter the impact of HLA-B*3501 in HIV infection. This is consistent with previous findings that increasing Gag-specific $CD8^+$ T-cell breadth is correlated with increasing viral suppression (39) and that the p24 Gag protein is infrequently targeted by HLA-B*3501-restricted $CD8^+$ T-cell responses in B-clade infection (67). These data also support previous studies that have suggested that even one effective CTL response can mediate long-term immune control of immunodeficiency virus infection, such as the KK10 (Gag positions 263 to 272) response in HIV-infected subjects with HLA-B*27 (27) or the SW9 (Gag positions 241 to 249) response in simian immunodeficiency virus (SIV)-infected Burmese macaques expressing the MHC 90-120-Ia haplotype (35, 70).

These data show that inadequate HLA-B*3501 binding of the peptide, as opposed to TcR paucity, as has been proposed as a mechanism for HLA-B*3501-associated rapid progression (41), may provide the explanation for the lack of a response to NY10-260E in B-clade infection. The two hypotheses are not mutually exclusive, and it remains possible that HLA-B*3501 is associated with some degree of protection against C-clade progression in spite of TcR paucity. However, the distinction is of direct relevance to vaccine design, since we show here that HLA-associated disease outcome is dependent on the epitopes being targeted, irrespective of any deficiencies attributed to the respective HLA molecule. Furthermore, it is striking that HLA-B*0702 and HLA-B*3501, the two alleles proposed to predispose to rapid HIV progression as a result of TcR paucity (41), both have a more successful impact on the viral set point in C-clade infection (Fig. 1), as do many other alleles within the HLA-B7 supertype whose peptide-binding motifs are very similar, namely, HLA-B*8101, B*4201, B*0705, and B*3910 (45).

These studies also draw attention to caveats associated with epitope prediction approaches using peptide-binding motifs or even those using the most sophisticated software that takes account of the possible contribution to MHC binding of every amino acid of every peptide known to bind to a particular MHC class I molecule. Although PPIPVGDIY (PY9) has appeared in the "A" list of HIV-specific $CD8^+$ T-cell epitopes since 1995 (48) and epitope prediction programs predict that PY9 would bind better than NY10 to HLA-B*3501 (17), nonetheless PY9 is not the epitope. It is significant that 0/377 peptides eluted from HLA class I molecules and sequenced have Pro at P1 (44). Bearing in mind the specificity of ERAP-1, which cleaves neither at X-P nor at P-X bonds (32), it seems that epitopes carrying Pro at P1, if they exist at all, are rare. The importance of defining the precise optimal epitope correctly is underlined by this study, in the demonstration that the 10-mer NY10 could only be immunogenic with Asp at P8 (Fig. 5). In contrast, although PY9-260E bound with stronger avidity than PY9-260D to HLA-B*3501, neither version of the 9-mer PY9 appeared to bind HLA-B*3501 with adequate stability to be immunogenic. It may be helpful in the future to confirm the identification of novel epitopes using peptide-MHC I tetramers, as now can be done readily (40, 43).

The critical contribution to MHC binding of the residue at P8 in an HLA-B*3501-restricted epitope was unexpected, given the peptide-binding motif of HLA-B*3501, which describes proline at P2 and Tyr at PC as the primary anchor residues, with various residues less strongly preferred at P2, P3, P4, and PC (18, 33). Explanation of this awaits the solution of the crystal structure of the HLA-B*3501–NY10-260D complex. However, an HLA-B*3501-EBV epitope structure has been solved (71), and modeling the HLA-B*3501-NY10 structure based on these data suggests that Asp at P8 in the NY10 epitope indeed points into the groove (Fig. 7). The model suggests that replacement of Asp by Glu at P8 would lead to steric hindrance between the longer side chain of Glu and the side chain of Ala-150 in the MHC α2 helix. The resulting altered conformation of the peptide would explain the observed reduction in stability of NY10-260E (Fig. 6B). This is consistent with the reduced but detectable processing of the NY10-260E peptide (data not shown) and is directly explained by the reduced affinity to the MHC molecule and thereby suggests that the limiting step in processing of the NY10-260E peptide occurs when the fully trimmed epitope is loaded onto the HLA-B*3501 molecule by the peptide-loading complex. This reduction in processing of the NY10-260E epitope may be critical to distinguish immunogenicity, especially at low infection levels of pri-

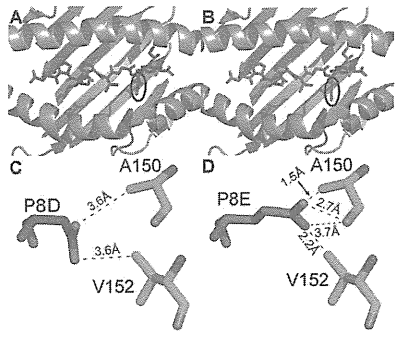

FIG 7 Modeled B3501-NY10 structure using the B3501-EPLPQGQLTAY complex (71). (A) HLA-B*3501 (shown in gray cartoon)-NPPIPVGDIY (shown in blue sticks), looking down at the MHC-binding groove. Position P8D in the peptide is circled. (B) HLA-B*3501 (shown in gray cartoon)-NPP IPVGEIY (shown in red sticks), looking down at the MHC-binding groove. P8E is circled. (C) Modeled interaction with NY10 residue P8D (blue stick) and MHC residues A150 and V152 (green sticks). (D) Modeled interaction with NY10 residue P8E (red stick) and MHC residues A150 and V152 (green sticks). The longer side chain of E in the escape mutant NY10 compared to D in the wild-type NY10 could generate steric hindrance with MHC residue A150. This could destabilize, and change the conformation of, the NY10 escape mutant peptide.

mary $CD4^+$ T cells *in vivo*, in contrast to the higher multiplicity of infection used *in vitro* in this assay.

The high frequency (~75%) of the D260E selection in C-clade infection suggests a highly functional Gag NY10-specific $CD8^+$ T-cell response *in vivo*. However, when we undertook sequencing of the Gag NY10 region from position 253 to 262 of 17 HLA-B*3501-positive recipients with known Gag NY10 sequences of their linked donor viruses, we did not find any selection of D260E escape mutation at very early viral load set points (CD4 count nadir) in 10 HLA-B*3501 individuals infected with the 260D virus (0/10) (data not shown). This suggests that the D260E selection occurs after the CD4 nadir during chronic infection and that the Gag NY10 response therefore may operate during chronic infection rather than during acute infection. This is consistent with a previous study showing that the HLA-B*3501-D260E mutation is selected outside acute infection (54). Moreover, we did not observe any change in the viral load set point for individuals carrying 260D versus 260E within linked recipients (37,720 versus 39,740 RNA copies/ml plasma; $P = 0.6$) early after infection or during chronic infection (17,550 versus 26,600 RNA copies/ml plasma; $P = 0.58$) (data not shown). However, the small numbers in combination with the potential compensatory mutations identified, which may restore viral fitness, may mask differences in viral load set point.

Although the residue at Gag-260 appears to play an important part in immunogenicity of the HLA-B*35:01-NY10 epitope, it is also important to note that, as with many amino acid substitutions in p24 Gag, this single-amino-acid substitution at Gag-260 is often observed in association with a number of other variations elsewhere in p24 Gag. In a covariation analysis (14), we identified 9 statistically significant associations ($q < 0.05$) between Gag-260D and variation at other positions (see Table S3 in the supplemental material), which may indicate that the D260E escape in C-clade virus may require compensatory mutations to minimize the impact on viral replicative capacity.

One further observation with respect to epitope definition highlighted by this study is the value of using a panel of overlapping peptides to comprehensively map responses made by HIV-infected subjects, as opposed to using epitope prediction. The other p24 Gag epitope defined here in HLA-B*3501-positive subjects, HPVHAGPIA (HA9), may have gone unnoticed previously because HLA-B*3501 typically shows a binding preference for Tyr or a larger hydrophobic residue than Ala at the C terminus. Between 40 and 60% of subjects studied here with HLA-B*3501 made a response to HA9, and, like for the NY10 Gag response, responders had significantly lower viral loads than nonresponders. Thus, a critical epitope within p24 Gag would have remained undetected had we used an approach based on predicted epitopes only.

Of note, we unexpectedly showed that a response to one of the Nef epitopes, NY8, was also associated with a lowered viremia in both B- and C-clade infection. $CD8^+$ T-cell responses to Nef have not typically been associated with disease control (39), but the data presented here suggest that specific responses within Nef may also mediate viremic suppression. In a previous study, it was observed that a substantial number of the Nef escape mutations revert following transmission to an HLA-mismatched host (54), suggesting a cost to viral fitness; the escape polymorphism itself may therefore contribute to disease control via an effect on viral replicative capacity. This finding is also consistent with data describing effective control of SIV in Mamu-B*08- and Mamu-B*17-positive rhesus macaques, which tend to target dominant epitopes not in Gag but in proteins such as Nef and Vif (49, 57). Thus, although a broad Gag-specific $CD8^+$ T-cell response may be more likely to be effective against HIV, it remains possible that $CD8^+$ T-cell responses targeting epitopes in non-Gag proteins may also be effective in containment of immunodeficiency virus infection.

It is important also to consider the limitations of this study. In particular, attention should be drawn to the fact that optimal HLA-B*3501-restricted epitopes 8 to 11 amino acids in length were tested for recognition in the B-clade-infected Japanese study subjects, whereas the C-clade-infected subjects were tested for recognition of the 18-mer overlapping peptides containing those optimal epitopes. Although responses to the 18-mer and to the optimal epitope have been strongly correlated (16) ($r = 0.85$; $P < 0.0001$ [H. N. Kloverpris et al., unpublished data]), the magnitude of response to the 18-mer tends to be somewhat lower than that to the optimal epitope, particularly if the location of the optimal epitope is in the central part of the 18-mer peptide (16, 55). However, this likely underestimation of the responses in the C-clade-infected study subjects, where response frequencies were determined using the 18-mer overlapping peptides, would likely have reduced the estimates of the frequency of Gag NY10 responses and of Gag HA9 responses, detected in 38% and 52% of subjects, respectively. Therefore, the difference in targeting of p24 Gag epitopes that exists between B- and C-clade-infected subjects is likely, if anything, to be even greater than shown in Fig. 4.

In summary, the impact of HLA alleles such as HLA-B*3501 on HIV disease outcome differs according to clade of infection. These data suggest that the critical difference in C-clade infection is the ability of HLA-B*3501-positive subjects to make two p24 Gag-specific responses restricted by this allele, NY10 and HA9, compared to only one (HA9) in B-clade-infected subjects. This result provides the clearest data yet that HLA-associated disease outcome is dependent on the epitopes being targeted, irrespective of

the nature of the restricting HLA molecule (55), and this provides hope that a vaccine that can induce effective $CD8^+$ T-cell responses can successfully bring about immune control even in people who carry HLA alleles traditionally regarded as associated with rapid disease progression.

ACKNOWLEDGMENTS

We declare that no competing interests exist.

This work was supported by the Welcome Trust (P.J.R.G.), National Institutes of Health grant R01 AI46995, and the Global COE program "Global Education and Research Center Aiming at the Control of AIDS," launched as a project commissioned by the Ministry of Education, Science, Sports, and Culture, Japan.

REFERENCES

1. Reference deleted.
2. **Alter G, Altfeld M.** 2009. NK cells in HIV-1 infection: evidence for their role in the control of HIV-1 infection. J. Intern. Med. **265**:29–42.
3. **Alter G, et al.** 2011. HIV-1 adaptation to NK-cell-mediated immune pressure. Nature **476**:96–100.
4. **Altfeld M, et al.** 2003. Influence of HLA-B57 on clinical presentation and viral control during acute HIV-1 infection. AIDS **17**:2581–2591.
5. **Altfeld M, Goulder P.** 2007. 'Unleashed' natural killers hinder HIV. Nat. Genet. **39**:708–710.
6. **Avila-Rios S, et al.** 2011. National prevalence and trends of HIV transmitted drug resistance in Mexico. PLoS One **6**:e27812. doi:10.1371/journal.pone.0027812.
7. **Bansal A, et al.** 2007. Immunological control of chronic HIV-1 infection: HLA-mediated immune function and viral evolution in adolescents. AIDS **21**:2387–2397.
8. Reference deleted.
9. Reference deleted.
10. **Brumme ZL, et al.** 2008. Human leukocyte antigen-specific polymorphisms in HIV-1 Gag and their association with viral load in chronic untreated infection. AIDS **22**:1277–1286.
11. **Carlson JM, et al.** 2008. Phylogenetic dependency networks: inferring patterns of CTL escape and codon covariation in HIV-1 Gag. PLoS Comput. Biol. **4**:e1000225. doi:10.1371/journal.pcbi.1000225.
12. **Carrington M, et al.** 1999. HLA and HIV-1: heterozygote advantage and B*35-Cw*04 disadvantage. Science **283**:1748–1752.
13. **Crawford H, et al.** 2009. Evolution of HLA-B*5703 HIV-1 escape mutations in HLA-B*5703-positive individuals and their transmission recipients. J. Exp. Med. **206**:909–921.
14. **Crawford H, et al.** 2011. The hypervariable HIV-1 capsid protein residues comprise HLA-driven CD8+ T-cell escape mutations and covarying HLA-independent polymorphisms. J. Virol. **85**:1384–1390.
15. **Crawford H, et al.** 2007. Compensatory mutation partially restores fitness and delays reversion of escape mutation within the immunodominant HLA-B*5703-restricted Gag epitope in chronic human immunodeficiency virus type 1 infection. J. Virol. **81**:8346–8351.
16. **Draenert R, et al.** 2003. Comparison of overlapping peptide sets for detection of antiviral CD8 and CD4 T cell responses. J. Immunol. Methods **275**:19–29.
17. **Erup Larsen M, et al.** 2011. HLArestrictor—a tool for patient-specific predictions of HLA restriction elements and optimal epitopes within peptides. Immunogenetics **63**:43–55.
18. **Falk K, et al.** 1993. Peptide motifs of HLA-B35 and -B37 molecules. Immunogenetics **38**:161–162.
19. **Fellay J, et al.** 2009. Common genetic variation and the control of HIV-1 in humans. PLoS Genet. **5**:e1000791. doi:10.1371/journal.pgen.1000791.
20. **Fellay J, et al.** 2007. A whole-genome association study of major determinants for host control of HIV-1. Science **317**:944–947.
21. **Flores-Villanueva PO, et al.** 2003. Associations of MHC ancestral haplotypes with resistance/susceptibility to AIDS disease development. J. Immunol. **170**:1925–1929.
22. **Flores-Villanueva PO, et al.** 2001. Control of HIV-1 viremia and protection from AIDS are associated with HLA-Bw4 homozygosity. Proc. Natl. Acad. Sci. U. S. A. **98**:5140–5145.
23. **Frahm N, et al.** 2006. Control of human immunodeficiency virus replication by cytotoxic T lymphocytes targeting subdominant epitopes. Nat. Immunol. **7**:173–178.
24. **Frahm N, et al.** 2004. Consistent cytotoxic-T-lymphocyte targeting of immunodominant regions in human immunodeficiency virus across multiple ethnicities. J. Virol. **78**:2187–2200.
25. **Gao X, et al.** 2001. Effect of a single amino acid change in MHC class I molecules on the rate of progression to AIDS. N. Engl. J. Med. **344**:1668–1675.
26. Reference deleted.
27. **Goulder PJ, et al.** 1997. Late escape from an immunodominant cytotoxic T-lymphocyte response associated with progression to AIDS. Nat. Med. **3**:212–217.
28. **Goulder PJ, Watkins DI.** 2008. Impact of MHC class I diversity on immune control of immunodeficiency virus replication. Nat. Rev. Immunol. **8**:619–630.
29. **Harndahl M, et al.** 2009. Peptide binding to HLA class I molecules: homogenous, high-throughput screening, and affinity assays. J. Biomol. Screen. **14**:173–180.
30. **Harndahl M, Rasmussen M, Roder G, Buus S.** 2011. Real-time, high-throughput measurements of peptide-MHC-I dissociation using a scintillation proximity assay. J. Immunol. Methods **374**:5–12.
31. **Harndahl M, et al.** 2012. Peptide-MHC class I stability is a better predictor than peptide affinity of CTL immunogenicity. Eur. J. Immunol. **42**:1405–1416.
32. **Hearn A, York IA, Rock KL.** 2009. The specificity of trimming of MHC class I-presented peptides in the endoplasmic reticulum. J. Immunol. **183**:5526–5536.
33. **Hill AV, et al.** 1992. Molecular analysis of the association of HLA-B53 and resistance to severe malaria. Nature **360**:434–439.
34. **Huang J, et al.** 2009. HLA-B*35-Px-mediated acceleration of HIV-1 infection by increased inhibitory immunoregulatory impulses. J. Exp. Med. **206**:2959–2966.
35. **Ishii H, et al.** 2012. Impact of vaccination on cytotoxic T lymphocyte immunodominance and cooperation against simian immunodeficiency virus replication in rhesus macaques. J. Virol. **86**:738–745.
36. **Itoh Y, et al.** 2005. High-throughput DNA typing of HLA-A, -B, -C, and -DRB1 loci by a PCR-SSOP-Luminex method in the Japanese population. Immunogenetics **57**:717–729.
37. **Kawashima Y, et al.** 2009. Adaptation of HIV-1 to human leukocyte antigen class I. Nature **458**:641–645.
38. **Kiepiela P, et al.** 2004. Dominant influence of HLA-B in mediating the potential co-evolution of HIV and HLA. Nature **432**:769–775.
39. **Kiepiela P, et al.** 2007. CD8+ T-cell responses to different HIV proteins have discordant associations with viral load. Nat. Med. **13**:46–53.
40. **Kloverpris HN, et al.** 2012. HLA-B*57 micropolymorphism shapes HLA allele-specific epitope immunogenicity, selection pressure, and HIV immune control. J. Virol. **86**:919–929.
41. **Kosmrlj A, et al.** 2010. Effects of thymic selection of the T-cell repertoire on HLA class I-associated control of HIV infection. Nature **465**:350–354.
42. **Lazaryan A, et al.** 2011. The influence of human leukocyte antigen class I alleles and their population frequencies on human immunodeficiency virus type 1 control among African Americans. Hum. Immunol. **72**:312–318.
43. **Leisner C, et al.** 2008. One-pot, mix-and-read peptide-MHC tetramers. PLoS One **3**:e1678. doi:10.1371/journal.pone.0001678.
44. **Leslie A, et al.** 2010. Additive contribution of HLA class I alleles in the immune control of HIV-1 infection. J. Virol. **84**:9879–9888.
45. **Leslie A, et al.** 2006. Differential selection pressure exerted on HIV by CTL targeting identical epitopes but restricted by distinct HLA alleles from the same HLA supertype. J. Immunol. **177**:4699–4708.
46. **Leslie AJ, et al.** 2004. HIV evolution: CTL escape mutation and reversion after transmission. Nat. Med. **10**:282–289.
47. **Listgarten J, et al.** 2008. Statistical resolution of ambiguous HLA typing data. PLoS Comput. Biol. **4**:e1000016. doi:10.1371/journal.pcbi.1000016.
48. **Llano A, Frahm N, Brander C.** 2009. How to optimally define optimal cytotoxic T lymphocyte epitopes in HIV infection? *In* Yusim K (ed), HIV molecular immunology 2009. Los Alamos National Laboratory, Los Alamos, NM.
49. **Loffredo JT, et al.** 2008. Patterns of CD8+ immunodominance may influence the ability of Mamu-B*08-positive macaques to naturally control simian immunodeficiency virus SIVmac239 replication. J. Virol. **82**:1723–1738.
50. **Marsh SGE, Parham P, Barber LD.** 2000. The HLA facts book. Academic Press, London, United Kingdom.

51. **Martin MP, et al.** 2002. Epistatic interaction between KIR3DS1 and HLA-B delays the progression to AIDS. Nat. Genet. **31**:429–434.
52. **Martin MP, et al.** 2007. Innate partnership of HLA-B and KIR3DL1 subtypes against HIV-1. Nat. Genet. **39**:733–740.
53. **Martinez-Picado J, et al.** 2006. Fitness cost of escape mutations in p24 Gag in association with control of human immunodeficiency virus type 1. J. Virol. **80**:3617–3623.
54. **Matthews PC, et al.** 2008. Central role of reverting mutations in HLA associations with human immunodeficiency virus set point. J. Virol. **82**: 8548–8559.
55. **Mothe B, et al.** 2011. Definition of the viral targets of protective HIV-1-specific T cell responses. J. Transl. Med. **9**:208.
56. **Mothe B, et al.** 2012. CTL responses of high functional avidity and broad variant cross-reactivity are associated with HIV control. PLoS One 7:e29717. doi:10.1371/journal.pone.0029717.
57. **Mothe BR, et al.** 2002. Characterization of the peptide-binding specificity of Mamu-B*17 and identification of Mamu-B*17-restricted epitopes derived from simian immunodeficiency virus proteins. J. Immunol. **169**: 210–219.
58. **Ngumbela KC, et al.** 2008. Targeting of a CD8 T cell env epitope presented by HLA-B*5802 is associated with markers of HIV disease progression and lack of selection pressure. AIDS Res. Hum. Retroviruses **24**:72–82.
59. **O'Brien SJ, Gao X, Carrington M.** 2001. HLA and AIDS: a cautionary tale. Trends Mol. Med. **7**:379–381.
60. **Payne RP, et al.** 2010. Efficacious early antiviral activity of HIV Gag- and Pol-specific HLA-B*2705-restricted CD8+ T-cells. J. Virol. **84**:10543–10557.
61. **Pereyra F, et al.** 2010. The major genetic determinants of HIV-1 control affect HLA class I peptide presentation. Science **330**:1551–1557.
62. **Prendergast A, et al.** 2010. HIV-1 infection is characterized by profound depletion of CD161+ Th17 cells and gradual decline in regulatory T cells. AIDS **24**:491–502.
63. **Rousseau CM, et al.** 2008. HLA class-I driven evolution of human immunodeficiency virus type 1 subtype C proteome: immune escape and viral load. J. Virol. **82**:6434–6446.
64. **Rowland-Jones S, et al.** 1995. HIV-specific cytotoxic T-cells in HIV-exposed but uninfected Gambian women. Nat. Med. **1**:59–64.
65. **Schneidewind A, et al.** 2007. Escape from the dominant HLA-B27-restricted cytotoxic T-lymphocyte response in Gag is associated with a dramatic reduction in human immunodeficiency virus type 1 replication. J. Virol. **81**:12382–12393.
66. **Shapiro RL, et al.** 2010. Antiretroviral regimens in pregnancy and breast-feeding in Botswana. N. Engl. J. Med. **362**:2282–2294.
67. **Streeck H, et al.** 2007. Recognition of a defined region within p24 gag by CD8+ T cells during primary human immunodeficiency virus type 1 infection in individuals expressing protective HLA class I alleles. J. Virol. **81**:7725–7731.
68. **Thananchai H, et al.** 2007. Allele-specific and peptide-dependent interactions between KIR3DL1 and HLA-A and HLA-B. J. Immunol. **178**:33–37.
69. **Tomiyama H, et al.** 1997. Evidence of presentation of multiple HIV-1 cytotoxic T lymphocyte epitopes by HLA-B*3501 molecules that are associated with the accelerated progression of AIDS. J. Immunol. **158**:5026–5034.
70. **Tsukamoto T, et al.** 2009. Impact of cytotoxic-T-lymphocyte memory induction without virus-specific CD4+ T-cell help on control of a simian immunodeficiency virus challenge in rhesus macaques. J. Virol. **83**:9339–9346.
71. **Tynan FE, et al.** 2007. A T cell receptor flattens a bulged antigenic peptide presented by a major histocompatibility complex class I molecule. Nat. Immunol. **8**:268–276.
72. **Ueno T, Idegami Y, Motozono C, Oka S, Takiguchi M.** 2007. Altering effects of antigenic variations in HIV-1 on antiviral effectiveness of HIV-specific CTLs. J. Immunol. **178**:5513–5523.
73. **Ueno T, et al.** 2008. CTL-mediated selective pressure influences dynamic evolution and pathogenic functions of HIV-1 Nef. J. Immunol. **180**:1107–1116.
74. **Westrop SJ, Grageda N, Imami N.** 2009. Novel approach to recognition of predicted HIV-1 Gag B3501-restricted CD8 T-cell epitopes by HLA-B3501(+) patients: confirmation by quantitative ELISpot analyses and characterisation using multimers. J. Immunol. Methods **341**: 76–85.

INTERNAL MEDICINE

CASE REPORT

Drug-Induced Acute Interstitial Nephritis Mimicking Acute Tubular Necrosis after Initiation of Tenofovir-Containing Antiretroviral Therapy in Patient with HIV-1 Infection

Takeshi Nishijima[1,5], Hirohisa Yazaki[1], Fumihiko Hinoshita[2], Daisuke Tasato[1,4], Kazufusa Hoshimoto[3], Katsuji Teruya[1], Hiroyuki Gatanaga[1,5], Yoshimi Kikuchi[1] and Shinichi Oka[1,5]

Abstract

We describe a case of 68-year-old Japanese man with HIV-1 infection who developed acute kidney injury with prominent tubular dysfunction immediately after starting tenofovir-containing antiretroviral therapy. Antiretroviral therapy was discontinued in two weeks but renal function, as well as tubular function, did not shown full recovery even at a 3-year follow-up examination. Acute tubular necrosis, a rare but well-known side effect of tenofovir, was suspected, but kidney biopsy confirmed interstitial nephritis. It is important to distinguish drug-induced interstitial nephritis from acute tubular necrosis, because early steroid administration can improve renal dysfunction caused by acute interstitial nephritis.

Key words: tenofovir, acute interstitial nephritis, acute tubular necrosis, acute kidney injury, HIV infection, kidney biopsy

(Intern Med 51: 2469-2471, 2012)
(DOI: 10.2169/internalmedicine.51.7766)

Introduction

Renal proximal tubular dysfunction is a well-known side effect of tenofovir (1, 2). Although rare, it sometimes leads to acute tubular necrosis (ATN) and results in acute kidney injury (AKI) (1, 3). Drug-induced acute interstitial nephritis has a similar clinical presentation to ATN, but has different etiology and management (4, 5). Here we report a case of tenofovir-induced acute interstitial nephritis (AIN) which mimicked ATN after initiation of tenofovir-containing antiretroviral therapy (ART).

Case Report

A 68-year-old Japanese man with history of hypertension and diabetes mellitus was diagnosed with HIV infection and pneumocystis pneumonia (PCP). The latter was treated with sulfamethoxazole/trimethoprim plus prednisolone for three weeks, and the patient was referred to our hospital. Reactivation of PCP occurred and he was again treated with sulfamethoxazole/trimethoprim for three weeks. After completion of PCP treatment, sulfamethoxazole/trimethoprim was replaced with atovaquone for secondary prophylaxis, and one month later ART was started with tenofovir/emtricitabine plus lopinavir/ritonavir (baseline CD4 count 39/μL, HIV viral load 990,000 copies/mL). Baseline renal function tests were within the normal range (serum creatinine 0.53 mg/dL, blood urea nitrogen 8.7 mg/dL) with urine β2 microglobulin (β2MG) of 2,327 μg/L. The concurrent drugs were atovaquone (which was switched to prophylactic dose of sulfamethoxazole/trimethoprim on ART day 2), azithro-

[1]AIDS Clinical Center, National Center for Global Health and Medicine, Japan, [2]Department of Nephrology, National Center for Global Health and Medicine, Japan, [3]Department of Pathology, National Center for Global Health and Medicine, Japan, [4]Department of Infectious, Respiratory, and Digestive Medicine Control and Prevention of Infectious Diseases, Faculty of Medicine, University of the Ryukyus, Japan and [5]Center for AIDS Research, Kumamoto University, Japan
Received for publication March 18, 2012; Accepted for publication June 14, 2012
Correspondence to Dr. Hiroyuki Gatanaga, higatana@acc.ncgm.go.jp

Intern Med 51: 2469-2471, 2012 DOI: 10.2169/internalmedicine.51.7766

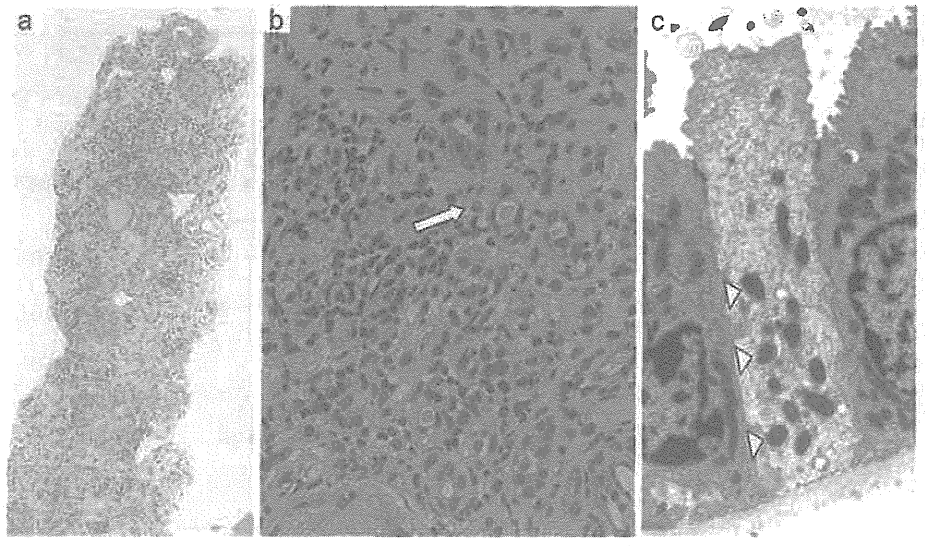

Figure 1. The microscopic findings in the renal biopsy specimen. (a) Diffuse interstitial inflammation with histologically normal glomeruli (Hematoxylin and Eosin (H&E) staining, ×10). (b) Prominent interstitial inflammatory infiltrates characterized by lymphocytes, plasma cells, and focal eosinophils (white arrow) (H&E staining, ×400). (c) Electron microscopic examination showed mitochondria normal in size and morphology in proximal tubular epithelial cells (white arrow heads) (×5,000).

mycin 1,200 mg/week, and olmesartan. No concurrent nonsteroidal anti-inflammatory drug was used.

Serum creatinine started to rise and on ART day 14, it reached 2.66 mg/dL with β2MG of 321,400 μg/L. No fever or rashes were observed, but prominent eosinophilia was noted (18.6% of leukocytes, 4,400/μL). Urine dipstick test showed proteinuria +3, occult blood +2, and glycosuria +1, together with renal tubular epithelial cells and granular casts in urine. Serum potassium, sodium, and phosphate levels were within the normal ranges. Serum IgE was high (1,040 IU/mL), and serum antinuclear antibodies, antineutrophil cytoplasm antibody, and cryoglobulin were negative. Renal ultrasonography was also negative for specific findings.

ART and the other concurrent medications, with the exception of azithromycin, were discontinued on that day. Hydration with central venous catheter was started. At 21 days after commencement of ART, serum creatinine reached a peak level of 5.39 mg/dL, though renal function started subsequently to improve slowly. At 32 days after discontinuation of ART, ART with darunavir/ritonavir plus raltegravir was provided (serum creatinine 2.59 mg/dL). The patient was discharged 44 days after re-commencement of ART with a CD4 count of 247/μL, and HIV viral load of 2,700 copies/mL. Within 3 months after discharge, HIV viral load was suppressed to <50 copies/mL with a CD4 count of 316/μL.

Five months after the episode, renal biopsy was performed (serum creatinine 1.76 mg/dL, β2MG 15,677 μg/L). Examination of the specimen showed interstitial infiltration of lymphocytes, plasma cells, and a few eosinophils. There was no vacuolation in tubular cells and the brush border was intact. The glomeruli were histologically normal (Fig. 1a, b). Immunofluorescence study was negative for IgG, IgM, IgA, C1q, C3, C4, or fibrinogen. Electron microscopic examination demonstrated no abnormalities in the mitochondria of tubular cells (Fig. 1c). The final diagnosis was drug-induced AIN. Serum creatinine and β2MG were still elevated three years later at 1.47 mg/dL and 25,718 μg/L, respectively.

Discussion

We described a case of tenofovir-induced AIN, which clinically mimicked ATN, after commencement of tenofovir-containing ART. Although the causative drugs were discontinued in two weeks, renal function did not show full recovery and the patient developed chronic kidney disease (Fig. 2). Tenofovir was highly likely the causative drug, because sulfamethoxazole/trimethoprim, the other drug which was used just before the occurrence of AIN, had been intermittently used for more than two months before the introduction of ART without any complications. To our knowledge, this is the fourth reported case of tenofovir-induced AIN, in addition to the three cases reported by Schmid et al. (6). Nevertheless, it is difficult to entirely role out the involvement of sulfamethoxazole/trimethoprim in occurrence of this AIN case. A combination effect of TDF and sulfamethoxazole/trimethoprim might have played a role.

It is difficult to diagnose interstitial nephritis based on clinical and laboratory findings only, and renal biopsy is required for a definitive diagnosis (4, 5). Only 5 to 10% of patients present with the classic triad of AIN symptoms: fever, rash, and eosinophilia (4, 5). However, renal biopsy is not performed in many cases with tenofovir-induced renal dysfunction, and thus, a considerable number of tenofovir-

Intern Med 51: 2469-2471, 2012 DOI: 10.2169/internalmedicine.51.7766

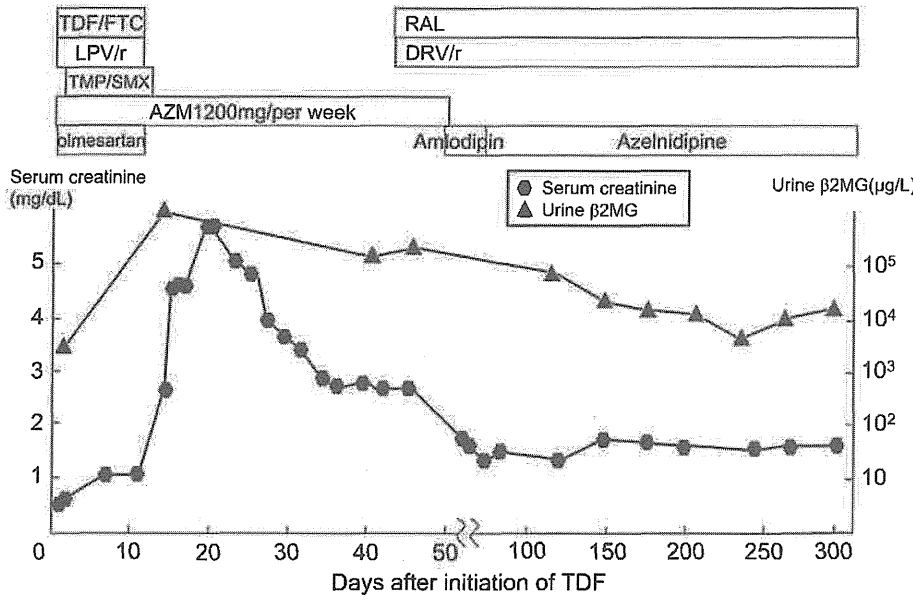

Figure 2. The clinical course of the patient. TDF/FTC: tenofovir/emtricitabine, LPV/r: ritonavir-boosted lopinavir, RAL: raltegravir, DRV/r: ritonavir-boosted darunavir, TMP/SMX: trimethoprim/sulfamethoxazole, AZM: azithromycin, β2MG: β2 microglobulin

induced AIN may have been misdiagnosed. Although a prominent eosinophilia and hyper-IgE (1,040 IU/mL) was noted for this case, these laboratory findings are commonly observed in patients with HIV-1 infection (7, 8). It is therefore difficult to dignose AIN solely based on these laboratory findings in patients with HIV infection.

The pathomechanism of tenofovir-induced ATN is considered to be mitochondrial toxicity in proximal tubular cells (9, 10). In contrast, interstitial nephritis occurs as an allergic response triggered by exposure to a drug (4, 5). It is important to distinguish AIN from ATN, because early steroid administration can improve the recovery of renal function in AIN (4, 5).

AIN should always be included in the differential diagnosis in a patient with AKI and prominent renal tubular damage following the introduction of tenofovir. In addition to prompt discontinuation of tenofovir, renal biopsy followed subsequently with steroid therapy at an early stage could produce a favorable renal outcome.

Author's disclosure of potential Conflicts of Interest (COI).
Oka S: Honoraria, Abbott Japan Co.; Research funding, MSD K. K..

Acknowledgement

The authors thank Makoto Mochizuki for the histopathological examination, and all the clinical staff at the AIDS Clinical Center for their excellent work.

All authors contributed to the concept, design, and writing of this submission.

References

1. Cooper RD, Wiebe N, Smith N, Keiser P, Naicker S, Tonelli M. Systematic review and meta-analysis: renal safety of tenofovir disoproxil fumarate in HIV-infected patients. Clin Infect Dis **51**: 496-505, 2010.
2. Rodriguez-Novoa S, Alvarez E, Labarga P, Soriano V. Renal toxicity associated with tenofovir use. Expert Opin Drug Saf **9**: 545-559, 2010.
3. Peyriere H, Reynes J, Rouanet I, et al. Renal tubular dysfunction associated with tenofovir therapy: report of 7 cases. J Acquir Immune Defic Syndr **35**: 269-273, 2004.
4. Praga M, Gonzalez E. Acute interstitial nephritis. Kidney Int **77**: 956-961, 2010.
5. Perazella MA, Markowitz GS. Drug-induced acute interstitial nephritis. Nat Rev Nephrol **6**: 461-470, 2010.
6. Schmid S, Opravil M, Moddel M, et al. Acute interstitial nephritis of HIV-positive patients under atazanavir and tenofovir therapy in a retrospective analysis of kidney biopsies. Virchows Arch **450**: 665-670, 2007.
7. Cohen AJ, Steigbigel RT. Eosinophilia in patients infected with human immunodeficiency virus. J Infect Dis **174**: 615-618, 1996.
8. Paganelli R, Scala E, Ansotegui IJ, et al. CD8+ T lymphocytes provide helper activity for IgE synthesis in human immunodeficiency virus-infected patients with hyper-IgE. J Exp Med **181**: 423-428, 1995.
9. Herlitz LC, Mohan S, Stokes MB, Radhakrishnan J, D'Agati VD, Markowitz GS. Tenofovir nephrotoxicity: acute tubular necrosis with distinctive clinical, pathological, and mitochondrial abnormalities. Kidney Int **78**: 1171-1177, 2010.
10. Kohler JJ, Hosseini SH, Hoying-Brandt A, et al. Tenofovir renal toxicity targets mitochondria of renal proximal tubules. Lab Invest **89**: 513-519, 2009.

Blunted fetal growth by tenofovir in late pregnancy

Tenofovir disoproxil fumarate (TDF) is recommended for pregnant women coinfected with HIV and hepatitis B virus to prevent mother-to-infant transmission of both viruses [1]. However, the safety of TDF in pregnancy is still controversial, especially with regard to its effects on fetal growth and bone mineralization.

Here, we describe a 32-year-old HIV-1-infected Asian pregnant woman, who showed blunted fetal growth during TDF treatment. She had been treated during the first 33 weeks of pregnancy with abacavir, lopinavir/ritonavir and raltegravir based on multiple viral mutations. As plasma concentrations of raltegravir were persistently low, treatment was switched to TDF at 35 weeks of gestation, until delivery at 38 weeks. The fetal growth curves of biparietal diameters and femur length were within the normal ranges before starting TDF; however, the growth of both parameters was significantly blunted after starting TDF (Fig. 1). Furthermore, tubular reabsorption rates for phosphate, urinary β2-microglobulin and alkaline phosphatase were 88%, 2776 μg/L and 435 U/L, respectively, during the TDF-treatment period, compared with 97%, 140 μg/L and 182 U/L, respectively, during the non-TDF-treatment period. Plasma TDF concentration in the mother was 3536 ng/mL at 4 h after dosing and 776 ng/mL in cord blood. The infant was delivered by cesarean section without HIV-1 infection, and weighed 2218 g (−2 SDs for Japanese infants), with a height of 45.0 cm (−1.5 SD), and a head circumference of 29.5 cm (−2 SD). Furthermore, moderate tubular dysfunction was observed at birth (serum calcium: 7.4 mg/dL, serum phosphate: 4.6 mg/dL, alkaline phosphatase: 560 U/L, urine β2-microglobulin: 1780 μg/L), together with a high plasma TDF concentration [102 ng/mL at 24 h after delivery (28 h after mother's dosing)]. Although the body length was persistently short throughout the first 3 months (less than −2 SD), the hand X-ray at 1 and 3 months showed no signs of osteopenia or rickets.

The present case raises two concerns with regard to the safety of TDF in pregnancy. TDF can reduce bone mineral density [2]. Van Rompay *et al.* [3] reported that treatment of infant macaque with high-dose TDF caused proximal tubular dysfunction, growth retardation and osteomalacia. Our findings suggest that administration of TDF during pregnancy caused fetal disordered bone growth through modest proximal tubular dysfunction. However, it is not clear whether maternal TDF-associated tubular dysfunction will cause future bone growth retardation in infants. A large cohort study reported that significantly shorter height was observed at age 1 year in TDF-exposed infants [4], which is generally considered as one of the symptoms of mild rickets. However, in our case, despite the persistently shorter height of the infant (less than −2 SD) throughout the first 3 months of life, hand X-ray at 3 months showed no findings of osteopenia or rickets. Second, plasma TDF concentrations in our case were 10-fold higher than the previously reported values [5], probably reflecting the mother's small body size (weight: 47 kg), and consequently higher placental transfer of TDF to the fetus. Asian pregnant women, who have smaller body size, may impose a more severe effect on fetal growth retardation than that reported previously. The effect of TDF in pregnancy and its impact on fetal growth needs to be evaluated in more detail.

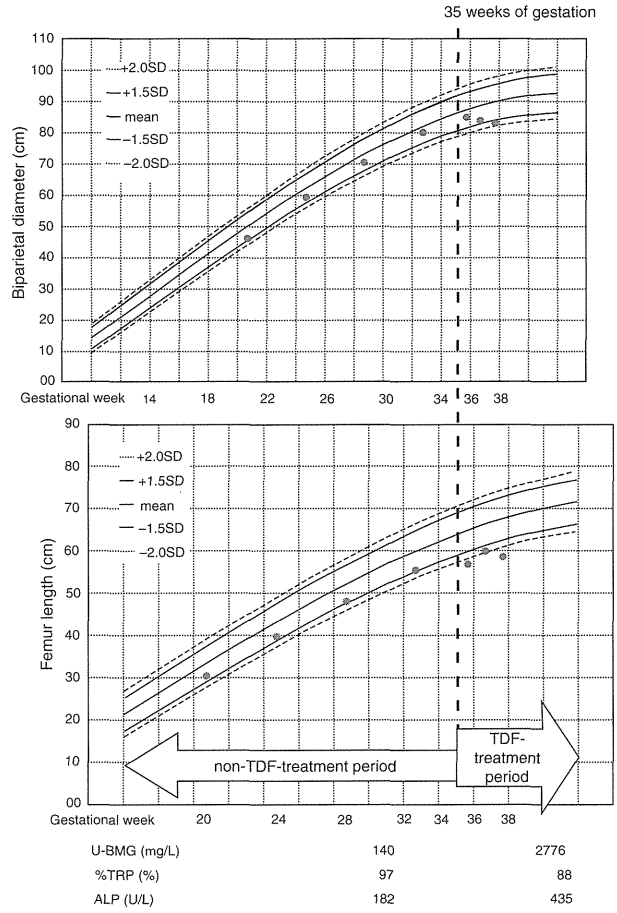

Fig. 1. Serial changes in fetal biparietal diameters, femur length and proximal tubular function during pregnancy. Between 20 and 33 weeks of gestation [non-tenofovir disoproxil fumarate (TDF)-treatment period], the growth curves of biparietal distance, femur length and proximal tubular function were within the normal ranges. However, the increases in biparietal distance and femur length were blunted after 35 weeks of gestation (TDF-treatment period), with a worsening of all markers of proximal tubular function. U-BMG, urine β2-microglobulin; %TRP, tubular reabsorption rate for phosphates; ALP, serum alkaline phosphatase.

Acknowledgements

Conflicts of interest

There are no conflicts of interest.

Ei Kinai[a], Shinichi Hosokawa[b], Hideto Gomibuchi[c], Hiroyuki Gatanaga[a], Yoshimi Kikuchi[a] and Shinichi Oka[a], *[a]AIDS Clinical Center, [b]Department of Pediatrics, and [c]Department of Obstetrics and Gynecology, National Center for Global Health and Medicine, Tokyo, Japan.*

Correspondence to Ei Kinai, MD, AIDS Clinical Center, National Center for Global Health and Medicine, Toyama 1-21-1, Shinjuku-ku, Tokyo, Japan.
Tel: +81 3 3202 7181; fax: +81 3 3202 7198;
e-mail: ekinai@acc.ncgm.go.jp

Received: 30 July 2012; accepted: 1 August 2012.

References

1. Panel on Treatment of HIV-Infected Pregnant Women and Prevention of Perinatal Transmission. Recommendations for Use of Antiretroviral Drugs in Pregnant HIV-1-Infected Women for Maternal Health and Interventions to Reduce Perinatal HIV Transmission in the United States. 2011. http://aidsinfo.nih.gov/ContentFiles/PerinatalGL.pdf.
2. McComsey GA, Kitch D, Daar ES, Tierney C, Jahed NC, Tebas P, *et al.* **Bone mineral density and fracrtures in antiretroviral naive persons randomized to receive abacavir-lamivudine or tenofovir disoproxil fumarate-emtricitabine along with efavirenz or atazanavir-ritonavir: AIDS clinical trials group A5224s, a substudy of ACTG A5202.** *J Infect Dis* 2011; **203**:1791–1801.
3. Van Rompay KKA, Brignolo LL, Meyer DJ, Jerome C, Tarara R, Spinner A, *et al.* **Biological effects of short-term or prolonged administration of 9-[2-(phosphonomethoxy) propyl] adenine (tenofovir) to newborn and infant rhesus macaques.** *Antimicrob Agents Chemother* 2004; **48**:1469–1487.
4. Siberry GK, Williams PL, Mendez H, Seage GR III, Jacobson DL, Hazra R, *et al.*, for the Pediatric HIV/AIDS Cohort Study (PHACS). **Safety of tenofovir use during pregnancy; early growth outcomes in HIV-exposed uninfected infants.** *AIDS* 2012, **26**:1151–1159.
5. Flynn PA, Mirochnick M, Shapiro DE, Bardequez A, Rodman J, Robbins B, *et al.*, PACTG 394 Study Team. **Pharmacokinetics and safety of single-dose tenofovir disoproxil fumarate and emtricitabine in HIV-1-infected pregnant women and their infants.** *Antimicrob Agents Chemother* 2011; **55**:5914–5922.

DOI:10.1097/QAD.0b013e328358ccaa

JVI Journals.ASM.org

Distinct HIV-1 Escape Patterns Selected by Cytotoxic T Cells with Identical Epitope Specificity

Yuichi Yagita,[a] Nozomi Kuse,[a] Kimiko Kuroki,[b] Hiroyuki Gatanaga,[a,c] Jonathan M. Carlson,[d] Takayuki Chikata,[a] Zabrina L. Brumme,[e,f] Hayato Murakoshi,[a] Tomohiro Akahoshi,[a] Nico Pfeifer,[d] Simon Mallal,[g] Mina John,[g] Toyoyuki Ose,[b] Haruki Matsubara,[b] Ryo Kanda,[b] Yuko Fukunaga,[b] Kazutaka Honda,[a] Yuka Kawashima,[a] Yasuo Ariumi,[a] Shinichi Oka,[a,c] Katsumi Maenaka,[b] Masafumi Takiguchi[a]

Center for AIDS Research, Kumamoto University, Chuo-ku, Kumamoto, Japan[a]; Laboratory of Biomolecular Science, Faculty of Pharmaceutical Sciences, Hokkaido University, Kita-ku, Sapporo, Japan[b]; AIDS Clinical Center, National Center for Global Health and Medicine, Shinjuku-ku, Tokyo, Japan[c]; eScience Group, Microsoft Research, Los Angeles, California[d]; Faculty of Health Sciences, Simon Fraser University, Burnaby BC, Canada[e]; British Columbia Centre for Excellence in HIV/AIDS, Vancouver, BC, Canada[f]; Institute for Immunology & Infectious Diseases, Murdoch University, Murdoch, Western Australia, Australia[g]

Pol283-8-specific, HLA-B*51:01-restricted, cytotoxic T cells (CTLs) play a critical role in the long-term control of HIV-1 infection. However, these CTLs select for the reverse transcriptase (RT) I135X escape mutation, which may be accumulating in circulating HIV-1 sequences. We investigated the selection of the I135X mutation by CTLs specific for the same epitope but restricted by HLA-B*52:01. We found that Pol283-8-specific, HLA-B*52:01-restricted CTLs were elicited predominantly in chronically HIV-1-infected individuals. These CTLs had a strong ability to suppress the replication of wild-type HIV-1, though this ability was weaker than that of HLA-B*51:01-restricted CTLs. The crystal structure of the HLA-B*52:01-Pol283-8 peptide complex provided clear evidence that HLA-B*52:01 presents the peptide similarly to HLA-B*51:01, ensuring the cross-presentation of this epitope by both alleles. Population level analyses revealed a strong association of HLA-B*51:01 with the I135T mutant and a relatively weaker association of HLA-B*52:01 with several I135X mutants in both Japanese and predominantly Caucasian cohorts. An *in vitro* viral suppression assay revealed that the HLA-B*52:01-restricted CTLs failed to suppress the replication of the I135X mutant viruses, indicating the selection of these mutants by the CTLs. These results suggest that the different pattern of I135X mutant selection may have resulted from the difference between these two CTLs in the ability to suppress HIV-1 replication.

HIV-1-specific cytotoxic T cells (CTLs) play an important role in the control of HIV-1 replication (1–8); however, they also select immune escape mutations (9, 10). Population level adaptation of HIV to human leukocyte antigen (HLA) has been demonstrated (11–15), suggesting that HIV-1 can successfully adapt to immune responses previously effective against it.

It is well known that particular mutations can be selected by CTLs specific for a single HIV-1 epitope. On the other hand, studies on HLA-associated HIV-1 polymorphisms have revealed examples of particular mutations associated with multiple HLA class I alleles (16–21), suggesting that the same mutation can be selected by CTLs carrying different specificities in some cases. However, the selection of the same mutation by CTLs specific for different HIV-1 epitopes has rarely been reported. The change from Ala to Pro at residue 146 of Gag (A146P) is a well-analyzed case. A146P is an escape selected by not only HLA-B*57-restricted, ISW9-specific CTLs (22) but also by HLA-B*15:10-restricted and HLA-B*48:01-restricted CTLs (15, 23, 24), although the latter CTLs selected it by different mechanisms. The replacement of Thr with Asn at residue 242 (T242N) of Gag is another case. This mutant is selected by HLA-B*58:01-restricted and HLA-B*57-restricted CTLs specific for the TW10 epitope in HIV-1 clade B- and C-infected individuals (25–27).

The presence of Pol283-8(TAFTIPSI: TI8)-specific, HLA-B*51:01-restricted CTLs is associated with low viral loads in HIV-1-infected Japanese hemophiliacs, supporting an important role in the long-term control of HIV-1 infection (28). We previously showed that the frequency of a mutation at position 135 (I135X) of reverse transcriptase (RT) is strongly correlated with the prevalence of HLA-B*51 among nine cohorts worldwide and that this mutation is selected by Pol283-8(TAFTIPSI: TI8)-specific, HLA-B*51:01-restricted CTLs (15). Of these cohorts, a Japanese one showed the highest frequency of the I135X mutation in HLA-B*51:01 negatives (66% in a Japanese cohort and 11 to 29% in other cohorts). This finding may be explained by the fact that the Japanese cohort has the highest prevalence of HLA-B*51:01 among these cohorts. Another possibility is that this mutation is selected by HIV-1-specific CTLs restricted by other HLA alleles, which are highly frequent among Japanese individuals but infrequent in or absent from other populations. To clarify the latter possibility, we first analyzed the association of the I135X mutation with other HLA class I alleles in a Japanese cohort and found this mutation also to be associated with HLA-B*52:01. We next sought to identify an HLA-B*52:01-restricted CTL epitope including RT135 and found that both HLA-B*51:01 and -B*52:01 can present the same epitope, Pol283-8. Using population level analyses of Japanese and Caucasian cohorts, we identified HLA-B*51:01- and HLA-B*52:01-specific polymorphisms at RT codon 135 (position 8 of this epitope) and characterized differential pathways of escape between these two alleles. In addition, we assessed the *in vitro* ability of HLA-B*52:01- and HLA-B*51:01-restricted CTLs to se-

Received 20 September 2012 Accepted 26 November 2012
Published ahead of print 12 December 2012
Address correspondence to Masafumi Takiguchi, masafumi@kumamoto-u.ac.jp.
Y.Y., N.K., and K.K. contributed equally to this study.
Supplemental material for this article may be found at http://dx.doi.org/10.1128/JVI.02572-12.

doi:10.1128/JVI.02572-12

lect I135X mutants and elucidated the crystal structure of the HLA-B*52:01-Pol283-8 peptide complex.

MATERIALS AND METHODS

Patients. Two hundred fifty-seven chronically HIV-1-infected, antiretroviral-naïve Japanese individuals were recruited for the present study, which was approved by the ethics committees of Kumamoto University and the National Center for Global Health and Medicine, Japan. Written informed consent was obtained from all subjects according to the Declaration of Helsinki.

In addition, HLA-associated immune selection pressure at RT codon 135 was investigated in the International HIV Adaptation Collaborative (IHAC) cohort, comprising >1,200 chronically HIV-infected, antiretroviral-naïve individuals from Canada, the United States, and Western Australia (19). The majority of the IHAC participants were Caucasian, and the HIV subtype distribution was >95% subtype B.

HIV-1 clones. An infectious proviral clone of HIV-1, pNL-432, and its mutant form pNL-M20A (containing a substitution of Ala for Met at residue 20 of Nef) were previously reported (29). Pol283-8 mutant viruses (Pol283-8L, -8T, -8V, and 8R) were previously generated on the basis of pNL-432 (15, 28).

Generation of CTL clones. Pol283-8-specific, HLA-B*52:01-restricted CTL clones were generated from HIV-1-specific, bulk-cultured T cells by limiting dilution in U-bottom 96-well microtiter plates (Nunc, Roskilde, Denmark). Each well contained 200 μl of the cloning mixture (about 1×10^6 irradiated allogeneic peripheral blood mononuclear cells (PBMCs) from healthy donors and 1×10^5 irradiated C1R-B*52:01 cells prepulsed with the corresponding peptide at 1 μM in RPMI 1640 supplemented with 10% human plasma and 200 U/ml human recombinant interleukin-2).

Intracellular cytokine staining (ICS) assay. PBMCs from HIV-1-seropositive HLA-B*52:01$^+$ HLA-B*51:01$^-$ individuals were cultured with each peptide (1 μM). Two weeks later, the cultured cells were stimulated with C1R-B*52:01 cells or those prepulsed with Pol283-8 peptide (1 μM) for 60 min, and then they were washed twice with RPMI 1640 containing 10% fetal calf serum (RPMI 1640-10% FCS). Subsequently, brefeldin A (10 μg/ml) was added. After these cells had been incubated for 6 h, they were stained with an anti-CD8 monoclonal antibody (MAb; Dako Corporation, Flostrup, Denmark), fixed with 4% paraformaldehyde, and then permeabilized with permeabilization buffer. Thereafter, the cells were stained with an anti-gamma interferon (IFN-γ) MAb (BD Bioscience). The percentage of CD8$^+$ cells positive for intracellular IFN-γ was analyzed by using a FACS-Cant II (BD Biosciences, San Jose, CA). All flow cytometric data were analyzed with FlowJo software (Tree Star, Inc., Ashland, OR).

Identification of 11-mer peptide recognized by HLA-B*52:01-restricted CD8$^+$ T cells. We identified an 11-mer peptide recognized by HLA-B*52:01-restricted CD8$^+$ T cells as follows. We stimulated PBMCs from a chronically HIV-1-infected HLA-B*52:01$^+$ donor (KI-069) with a peptide cocktail including overlapping 17-mer peptides covering RT135 and cultured the cells for 14 days. The cells in bulk culture were assessed by performing an ICS assay for C1R-HLA-B*52:01 cells prepulsed with each of these 17-mer peptides. The bulk-cultured cells recognized the target cells prepulsed with two of the 17-mer peptides assessed, Pol17-47 (KDFRKYTAFTIPSINNE) and Pol17-48 (TAFTIPSINNETPGIRT). Further analysis with 11-mer overlapping peptides covering the Pol17-48 sequence showed that these bulk-cultured cells recognized the target cells prepulsed with Pol11-142 (TAFTIPSINNE) but not those prepulsed with Pol11-143 (FTIPSINNETP).

Assay of cytotoxicity of CTL clones to target cells prepulsed with the epitope peptide or infected with a vaccinia virus–HIV-1 recombinant. The cytotoxicity of Pol283-8-specific, HLA-B*52:01-restricted CTL clones to C1R cells expressing HLA-B*52:01 (C1R-B*52:01), which were previously generated (30), and prepulsed with peptide or infected with a vaccinia virus-HIV-1Gag/Pol recombinant was determined by the standard ^{51}Cr release assay described previously (31). In brief, the infected cells were incubated with 150 μCi $Na_2{}^{51}CrO_4$ in saline for 60 min and then washed three times with RPMI 1640 medium containing 10% newborn calf serum. Labeled target cells (2×10^3/well) were added to each well of a U-bottom 96-well microtiter plate (Nunc, Roskilde, Denmark) with the effector cells at an effector-to-target (E/T) cell ratio of 2:1. The cells were then incubated for 6 h at 37°C. The supernatants were collected and analyzed with a gamma counter. Spontaneous ^{51}Cr release was determined by measuring the number of counts per minute (cpm) in supernatants from wells containing only target cells (cpm spn). Maximum ^{51}Cr release was determined by measuring the cpm in supernatants from wells containing target cells in the presence of 2.5% Triton X-100 (cpm max). Specific lysis was defined as (cpm exp − cpm spn)/(cpm max − cpm spn) × 100, where cpm exp is the number of cpm in the supernatant in the wells containing both target and effector cells.

Enzyme-linked immunospot (ELISPOT) assay. Cryopreserved PBMCs of chronically HIV-1-infected HLA-B*52:01$^+$ individuals were plated in 96-well polyvinylidene plates (Millipore, Bedford, MA) that had been precoated with 5 μg/ml anti-IFN-γ MAb 1-DIK (Mabtech, Stockholm, Sweden). The appropriate amount of each peptide (100 or 10 nM) was added in a volume of 50 μl, and then PBMCs were added at 1×10^5 cells/well in a volume of 100 μl. The plates were incubated for 40 h at 37°C in 5% CO_2 and then washed with phosphate-buffered saline (PBS) before the addition of biotinylated anti-IFN-γ MAb (Mabtech) at 1 μg/ml. After the plates had been incubated at room temperature for 100 min and then washed with PBS, they were incubated with streptavidin-conjugated alkaline phosphatase (Mabtech) for 40 min at room temperature. Individual cytokine-producing cells were detected as dark spots after a 20-min reaction with 5-bromo-4-chloro-3-indolylphosphate and nitroblue tetrazolium by using an alkaline phosphatase-conjugate substrate (Bio-Rad, Richmond, CA). The spots were counted by an Eliphoto-Counter (Minerva Teck, Tokyo, Japan). PBMCs without peptide stimulation were used as a negative control. Positive responses were defined as those greater than the mean of the negative-control wells plus 2 standard deviations (SD) (the number of spots in wells without peptides).

HIV-1 replication suppression assay. The ability of HIV-1-specific CTLs to suppress HIV-1 replication was examined as previously described (32). CD4$^+$ T cells isolated from PBMCs derived from an HIV-1-seronegative individual with HLA-B*52:01, HLA-B*51:01, or both were cultured. After the cells had been incubated with the desired HIV-1 clones for 4 h at 37°C, they were washed three times with RPMI 1640-10% FCS medium. The HIV-1-infected CD4$^+$ T cells were then cocultured with Pol283-8-specific CTL clones. From day 3 to day 7 postinfection, culture supernatants were collected and the concentration of p24 antigen (Ag) in them was measured by use of an enzyme-linked immunosorbent assay kit (HIV-1 p24 Ag ELISA kit; ZeptoMetrix).

HLA stabilization assay with RMA-S cells expressing HLA-B*52:01 or HLA-B*51:01. The peptide-binding activity of HLA-B*52:01 or HLA-B*51:01 was assessed by performing an HLA stabilization assay with RMA-S cells expressing HLA-B*52:01 (RMA-S-B*52:01) or HLA-B*51:01 (RMA-S-B*51:01) as described previously (33). Briefly, RMA-S-B*51:01 and RMA-S-B*52:01 cells were cultured at 26°C for 16 to 24 h. The cells (2×10^5) in 50 μl of RPMI 1640 supplemented with 5% FCS (RPMI–5% FCS) were incubated at 26°C for 3 h with 50 μl of a solution of peptides at 10^{-3} to 10^{-7} M and then at 37°C for 3 h. After having been washed with RPMI–5% FCS, the cells were incubated for 30 min on ice with an appropriate dilution of TP25.99 MAb. After two washings with RPMI–5% FCS, they were incubated for 30 min on ice with an appropriate dilution of fluorescein isothiocyanate (FITC)-conjugated anti-mouse Ig antibodies. Finally, the cells were washed three times with RPMI–5% FCS and the fluorescence intensity of the cells was measured by the FACS-Cant II. Relative mean fluorescence intensity (MFI) was calculated by subtracting the MFI of cells not peptide pulsed from that of the peptide-pulsed ones.

Sequencing of plasma RNA. Viral RNA was extracted from the plasma of chronically HIV-1-infected Japanese individuals by using a QIAamp

Mini Elute Virus spin kit (Qiagen). cDNA was synthesized from the RNA with Superscript II and random primer (Invitrogen). We amplified HIV RT and integrase sequences by nested PCR with RT-specific primers 5′-CCAAAAGTTAAGCAATGGCC-3′ and 5′-CCCATCCAAAGGAATGGAGG-3′ or 5′-CCTTGCCCCTGCTTCTGTAT-3′ for the first-round PCR and 5′-AGTTAGGAATACCACACCCC-3′ and 5′-GTAAATCCCCACCTCAACAG-3′ or 5′-AATCCCCACCTCAACAGAAG-3′ for the second-round PCR and integrase-specific primers 5′-ATCTAGCTTTGCAGGATTCGGG-3′ and 5′-CCTTAACCGTAGTACTGGTG-3′ or 5′-CCTGATCTCTTACCTGTCC-3′ for the first-round PCR and 5′-AAAGGTCTACCTGGCATGGG-3′ or 5′-TTGGAGAGCAATGGCTAGTG-3′ and 5′-AGTCTACTTGTCCATGCATGGC-3′ for the second-round PCR. PCR products were sequenced directly or cloned with a TOPO TA cloning kit (Invitrogen) and then sequenced. Sequencing was done with a BigDye Terminator v1.1. cycle sequencing kit (Applied Biosystems) and analyzed by an ABI PRISM 310 Genetic Analyzer.

Statistical analysis with phylogenetically corrected odds ratios. Strength of selection was measured by using a phylogenetically corrected odds ratio as previously described (19). Briefly, the odds of observing a given amino acid (e.g., 135V) was modeled as $P/(1-P) = (a \times X) + (b \times T)$, where P is the probability of observing 135V in a randomly selected individual, X is a binary (0/1) variable representing whether or not an individual expresses the HLA allele in question (e.g., B*52:01), and T equals 1 if the transmitted/founder virus for that individual carried 135V and −1 otherwise. Because the transmitted/founder virus is unknown, we averaged over all possibilities by using weights informed by a phylogeny that was constructed from the RT sequences of all of the individuals in the study. The parameters a and b were determined by using iterative maximum-likelihood methods. The maximum-likelihood estimate of a is an estimate of the natural logarithm of the odds ratio of observing 135V in individuals expressing X versus individuals not expressing X, conditioned on the individuals' (unobserved) transmitted/founder virus. P values are estimated by using a likelihood ratio test that compares the above model to a null model in which a equals 0.

To compare the odds of selection between two cohorts, we modified the phylogenetically corrected logistic regression model to include a cohort term, $Z = X \times Y$, where X is the HLA allele, and Y is a 0/1 variable that indicates cohort membership, yielding $P/(1-P) = (a \times X) + (b \times T) + (c \times Z)$, as previously described (19, 34). A P value testing if the odds of escape are different in the two cohorts was estimated by using a likelihood ratio test that compared this model to a null model where c equals 0.

Generation of HLA class I tetramers. HLA class I-peptide tetrameric complexes (tetramer) were synthesized as described previously (31, 35). The Pol283-8 peptide was used for the refolding of HLA-B*51:01 or HLA-B*52:01 molecules. Phycoerythrin (PE)-labeled streptavidin (Molecular Probes) was used for generation of the tetramers.

Tetramer binding assay. HLA-B*51:01-restricted and HLA-B*52:01-restricted CTL clones were stained at 37°C for 30 min with PE-conjugated HLA-B*51:01-tetramer and HLA-B*52:01-tetramer, respectively, at concentrations of 5 to 1,000 nM. After two washes with RPMI 1640 medium supplemented with 10% FCS (RPMI 1640–10% FCS), the cells were stained with FITC-conjugated anti-CD8 MAb at 4°C for 30 min, followed by 7-amino-actinomycin D at room temperature for 10 min. After two more washes with RPMI 1640–10% FCS, the cells were analyzed by the FACS-Cant II flow cytometer. The tetramer concentration that yielded the half-maximal MFI (the EC_{50}) was calculated by probit analysis.

Crystallization, data collection, and structure determination. Soluble HLA-B*52:01 (with beta-2 microglobulin and peptide TAFTIPSI) was prepared as described above. Prior to crystallization trials, HLA-B*52:01 was concentrated to a final concentration of 20 mg ml^{-1} in 20 mM Tris-HCl (pH 8.0) buffer containing 250 mM NaCl. This was done with a Millipore centrifugal filter device (Amicon Ultra-4, 10-kDa cutoff; Millipore). Screening for crystallization was performed with commercially available polyethylene glycol (PEG)-based screening kits, PEGs and PEGs II suites (Qiagen). Thin needle crystals were observed from PEGs II suite 23 (0.2 M sodium acetate, 0.1 M HEPES [pH 7.5], and 20% PEG 3000). Several conditions were further screened by the hanging-drop method with 24-well VDX plates (Hampton Research) by mixing 1.5 μl protein solution and 1.5 μl reservoir to be equilibrated against reservoir solution (0.5 ml) at 293 K. Best crystals were grown from macro seeding with the initial crystals obtained with 0.2 M sodium acetate, 0.1 M Bis Tris propane [pH 7.5], and 20% PEG 3350.

The data set was collected at beamline BL41XU of SPring-8 with Rayonix charge-coupled device detector MX225HE. Prior to diffraction data collection, crystals were cryoprotected by transfer to a solution containing 25% (vol/vol) glycerol and incubation in it for a few seconds, followed by flash cooling. The data sets were integrated with XDS (36) and then merged and scaled by using Scala (37). HLA-B*52:01 crystals belonged to space group $P2_12_12_1$, with unit cell parameters $a = 69.0$ Å, $b = 83.3$ Å, and $c = 170.3$ Å. Based on the values of the Matthews coefficient (V_M) (38), we estimated that there were two protomers in the asymmetric unit with a V_M value of 1.37 A^3/Da (Vsolv = 10.5%). For details of the data collection and processing statistics, see Table S1 in the supplemental material.

The structure was solved by the molecular replacement method with Molrep (39). The crystal structure of HLA-B*51:01 (PDB ID: 1E28) was used as a search model. Structure refinement was carried out by using Refmac5 (40) and phenix (41). The final model was refined to an Rfree factor of 34.7% and an R factor of 29.5% with a root mean square deviation of 0.014 Å in bond length and 1.48° in bond angle for all reflections between resolutions of 38.8 and 3.1 Å. Table S1 in the supplemental material also presents a summary of the statistics for structure refinement. The stereochemical properties of the structure were assessed by Procheck (42) and COOT (43) and showed no residues in the disallowed region of the Ramachandran plot.

Protein structure accession number. Atomic coordinates and structure factors for HLA-B*52:01 have been deposited in the Protein Data Bank under accession code 3W39.

RESULTS

Association of I135X variants with HLA-B*52:01. To clarify the possibility that CTLs restricted by other HLA alleles select the I135X mutation, we investigated the association between other HLA alleles and this mutation in 257 Japanese individuals chronically infected with HIV-1. We found an association of HLA-B*52:01 with the I135X variant, though this association was weaker than that with HLA-B*51:01 (phylogenetically corrected ln odds ratio [lnOR] of 11.76 [$P = 8.77 \times 10^{-4}$] for B*52:01 versus an lnOR of 40.0 [$P = 5.78 \times 10^{-12}$] for B*51:01; Table 1). We also analyzed the effects of HLA-B*52:01 and HLA-B*51:01 in chronically HIV-1-infected Japanese individuals, excluding HLA-B*51:01$^+$ and HLA-B*52:01$^+$ individuals, respectively, and found a significant association between HLA-B*52:01 and I135X variants among 200 HLA-B*51:01-negative individuals with chronic HIV-1 infection ($P = 4.7 \times 10^{-4}$; see Fig. S1A in the supplemental material) and that of HLA-B*51:01 with the variants in 202 HLA-B*52:01-negative ones ($P = 5.3 \times 10^{-8}$; see Fig. S1B in the supplemental material). These results together imply that HLA-B*52:01-restricted CTLs selected this mutation.

Identification of HLA-B*52:01-restricted, Pol283-specific CTLs. To identify the HLA-B*52:01-restricted HIV-1 epitope including RT135, we first investigated whether overlapping peptides covering RT135 could elicit CD8$^+$ T cells specific for these peptides in chronically HIV-1-infected individuals. We identified CTLs recognizing the Pol11-142 (TAFTIPSINNE) peptide in a chronically HIV-1-infected HLA-B*52:01$^+$ donor, KI-069 (see Materials and Methods). Since the C terminus of HLA-B*52:01-binding peptides is known to be a hydrophobic residue (30, 44), we speculated that TAFTIPSI (Pol283-8) was the epitope peptide.

TABLE 1 HLA-B*52:01 and HLA-B*51:01 association with variation at RT135 in Japanese and Caucasian cohorts

HLA class I allele	RT135 target variable	PlyloLOR[a]		Within-cohort *P* value		*P* value comparing cohorts
		Japanese	IHAC	Japanese	IHAC	
B*51:01	T	13.70	4.53	4.66×10^{-6}	1.70×10^{-35}	0.042
B*52:01	T	−9.77	1.25	0.464	2.04×10^{-3}	0.62
B*51:01	I	−40.00	−5.71	5.78×10^{-12}	1.58×10^{-51}	0.052
B*52:01	I	−11.76	−3.06	8.77×10^{-4}	2.95×10^{-5}	0.52
B*51:01	V	−9.76	8.52	0.884	0.41	0.85
B*52:01	V	12.21	10.15	0.076	1.82×10^{-3}	0.037
B*51:01	R	12.08	13.02	0.038	2.36×10^{-3}	0.42
B*52:01	R	0.26	8.37	0.423	0.469	0.89
B*51:01	L	−0.89	3.21	1	0.038	0.17
B*52:01	L	−0.56	3.61	1	0.231	0.29
B*51:01	K	−0.71	−40.00	1	0.53	0.99
B*52:01	K	−0.69	−40.00	1	0.779	0.99
B*51:01	M	7.76	12.00	0.894	2.10×10^{-4}	0.34
B*52:01	M	11.09	−40.00	0.034	0.517	0.12

[a] PlyloLOR, phylogenetically corrected lnOR.

Indeed, bulk-cultured T cells that had been cultured for 2 weeks after stimulation with Pol17-48 recognized C1R-B*52:01 cells prepulsed with Pol283-8 peptide at a much lower concentration than those incubated with the Pol11-142 peptide (Fig. 1A), strongly suggesting that Pol283-8 is an epitope recognized by HLA-B*52:01-restricted CTLs. These findings were confirmed by ELISPOT assay with PBMCs from two HLA-B*52:01$^+$ individuals chronically infected with HIV-1 (Fig. 1B). To clarify whether this peptide was processed and presented by HLA-B*52:01, we investigated the killing activity of bulk-cultured T cells against HLA-B*52:01$^+$ target cells infected with a vaccinia virus–HIV-1 Gag/Pol recombinant. They killed target cells infected with this recombinant but not those infected with wild-type vaccinia virus (Fig. 1C), indicating that the Pol283-8 peptide was presented by

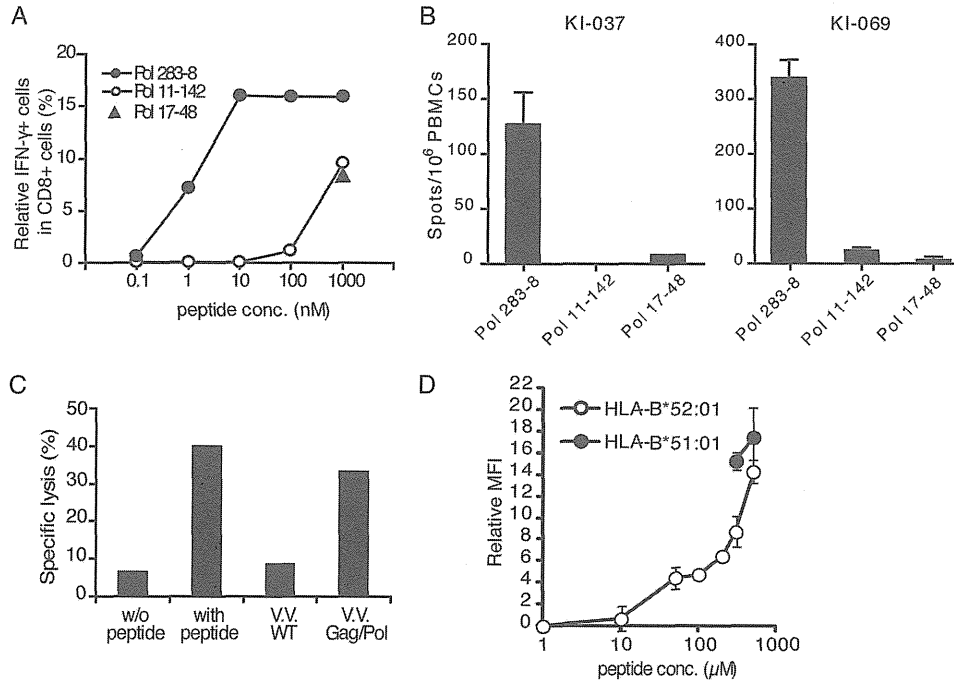

FIG 1 Identification of HLA-B*52:01-restricted Pol epitope. (A) Identification of the epitope peptide recognized by HLA-B*52:01-restricted CD8$^+$ T cells. Bulk T cells were cultured for 2 weeks after stimulation with the Pol17-48 peptide, and then the recognition of C1R-HLA-B*52:01 cells prepulsed with Pol17-48, Pol11-142, or Pol283-8 peptide was assessed by ICS assay. (B) Pol283-8 peptide recognition by T cells *ex vivo*. Recognition of the Pol17-48, Pol11-142, or Pol283-8 peptide by PBMCs from two HLA-B*52:01$^+$ individuals chronically infected with HIV-1 (KI-037 and KI-069) was analyzed by ELISPOT assay. A 100 nM concentration of each peptide was used. (C) Killing activity of Pol283-specific, HLA-B*52:01-restricted CD8$^+$ T cells against cells infected with a vaccinia virus–HIV-1 Gag/Pol recombinant. The killing activities of bulk-cultured T cells stimulated with Pol11-142 against target cells infected with a vaccinia virus–HIV-1 Gag/Pol recombinant (Gag/Pol) and against those infected with wild-type vaccinia virus (V.V. WT) are shown. (D) Binding of Pol283-8 peptide to HLA-B*52:01. Binding ability was measured by performing the HLA class I stabilization assay with RMA-S-B*52:01. RMA-S-B*51:01 cells were used as control cells for the Pol283-8 peptide.

TABLE 2 Pol283-8-specific CD8$^+$ T cells in chronically HIV-1-infected, HLA-B*52:01$^+$ individuals

Patient ID	HLA class I alleles		No. of CD4 cells/μl	No. of CD8 cells/μl	Viral load (no. of copies/ml)	Antiretroviral therapy	Relative IFN-γ$^+$/CD8$^+$ % in ICC assay	No. of spots/10^6 PBMCs in ELISPOT[a] assay
KI-037	A*24:02/−	B*52:01/40:02	465	973	76,000	−	64.1	150
KI-090	A*24:02/−	B*52:01/55:01	606	511	≤50	+	40.2	80
KI-106	A*24:02/33:03	B*52:01/07:01	433	890	≤50	+	1.4	<79
KI-126	A*24:02/31:01	B*52:01/40:01	465	NT[b]	36,000	−	60.4	<79
KI-130	A*24:02/−	B*52:01/07:02	351	1,275	14,000	−	0.0	<79
KI-167	A*24:02/−	B*52:01/54:01	455	909	26,000	−	0.0	<79
KI-067	A*24:02/−	B*52:01/48:01	234	1,198	89,000	−	10.9	<79
KI-071	A*24:02/31:01	B*52:01/40:06	292	1,134	48,000	−	0.7	<79
KI-076	A*02:01/24:01	B*52:01/40:01	136	252	14,000	−	61.0	80
KI-114	A*02:01/24:01	B*52:01/27:04	416	463	≤50	+	0.1	<79
KI-056	A*24:02/−	B*52:01/40:02	290	844	8,200	−	-0.1	<79
KI-108	A*24:02/−	B*52:01/−	373	481	NT	−	1.0	<79
KI-028	A*24:02/26:01	B*52:01/48:01	1,351	811	≤50	+	0.5	<79
KI-069	A*24:02/−	B*52:01/40:06	448	1,631	4,400	−	18.1	790

[a] More than the mean number of negative-control spots + 2 SD was defined as a positive response (positive response, >79 spots).
[b] NT, not tested.

HLA-B*52:01. We analyzed the binding of the Pol283-8 peptide to HLA-B*52:01 by using the HLA stabilization assay. The results demonstrated that this peptide bound to HLA-B*52:01 (Fig. 1D). These results together indicate that the Pol283-8 epitope can therefore be presented by both HLA-B*51:01 and HLA-B*52:01.

We investigated whether Pol283-8-specific CD8$^+$ T cells were elicited predominantly in chronically HIV-1-infected HLA-B*52:01$^+$ HLA-B*51:01$^-$ individuals. PBMCs from 14 of these individuals were analyzed by ICS assay with Pol283-8 peptide-stimulated culture cells, as well as by ELISPOT assay. The results of the ICS assay showed that 7 of these 14 HLA-B*52:01$^+$ HLA-B*51:01$^-$ patients had Pol283-specific CD8$^+$ T cells, whereas those of the ELISPOT assay with *ex vivo* PBMCs revealed that Pol283-specific CD8$^+$ T cells were detected in only four individuals (Table 2). These results suggest that the three individuals in whom the specific CTLs were detected by the ICS assay but not by the ELISPOT assay may have memory T cells. These results together indicate that Pol283-8 was recognized as an HLA-B*52:01-restricted immunodominant epitope in the HLA-B*52:01$^+$ individuals and support the idea that the I135X mutation was selected by HLA-B*52:01-restricted, Pol283-8-specific CD8$^+$ T cells.

Strong ability of HLA-B*52:01-restricted, Pol283-8-specific CD8$^+$ T cells to suppress HIV-1 replication. A previous study showed that HLA-B*51:01-restricted, Pol283-8-specific T cells have a strong ability to kill HIV-1-infected target cells and to suppress HIV-1 replication (31). Therefore, we expected that the HLA-B*52:01-restricted T cells also would have this strong ability. We generated HLA-B*52:01-restricted, Pol283-8-specific T cell clones and investigated their ability to kill peptide-pulsed or HIV-1-infected target cells. Clone 1E1 effectively killed C1R-B*52:01 cells prepulsed with the Pol283-8 peptide (Fig. 2A) and NL-432-infected CD4$^+$ T cells from an HLA-B*52:01$^+$ individual (Fig. 2B). Additional T cell clones also showed strong killing activity against NL-432-infected HLA-B*52:01$^+$ CD4$^+$ T cells (data not shown). In addition, we investigated the ability of these CTL clones to suppress HIV-1 replication. CD4$^+$ T cells derived from an HLA-B*52:01$^+$ individual were infected with NL-432 or M20A mutant virus, the latter of which has an amino acid substitution at position 20 of Nef and lacks the ability to downregulate the surface expression of HLA-A and -B molecules (Fig. 2C). Representative data on the 1E1 clone and summary data on four clones are shown in Fig. 2D and E, respectively. These CTL clones strongly suppressed the replication of both the NL432 and M20A mutant viruses, indicating that the HLA-B*52:01-restricted CTLs had a strong ability to suppress HIV-1 replication, as was the case with the HLA-B*51:01-restricted ones.

Recognition of I135X mutations by Pol283-8-specific, HLA-B*52:01-restricted CTLs. Four mutations (8T, 8L, 8R, and 8V) were observed predominantly at RT135 in chronically HIV-1-infected HLA-B*52:01$^+$ individuals (Fig. 3). These mutations may have been selected by Pol283-8-specific, HLA-B*52:01-restricted CTLs in these patients. We therefore investigated the ability of HLA-B*52:01-restricted CTLs to suppress the replication of these mutant viruses *in vitro*. The CTL clones failed to suppress the replication of the 8L, 8T, or 8R mutant, though they weakly suppressed that of the 8V virus at an E/T cell ratio of 1:1 (Fig. 4A). These results support the idea that these variants were escape mutations from the HLA-B*52:01-restricted CTLs. To clarify the mechanism by which the CTL clones failed to suppress the replication of these mutant viruses, we investigated the CTL clones for recognition of C1R-B*52:01 cells prepulsed with the mutant peptides. The CTL clones effectively recognized the 8V peptide at the same level as the wild-type peptide and the 8T and 8L peptides at less than that of the wild-type one, whereas they failed to recognize the 8R peptide (Fig. 4B). An ELISPOT assay with *ex vivo* PBMCs from KI-069 showed that Pol283-8-specific CTLs effectively recognized the 8I and 8V variants but not the other three mutant peptides (Fig. 4C), suggesting that Pol283-8-specific CTLs failed to recognize the 8T, 8L, and 8R peptides *in vivo*. The lack of recognition of these mutants by CTLs may be attributable to a failure of T cell receptor (TCR) recognition, the inability of the peptide to bind to HLA-B*52:01, and/or disruption of the processing of the epitope in HIV-1-infected cells.

Different pattern of RT135 mutation selection by two HLA alleles. As described above, HLA-B*51:01 and HLA-B*52:01 were associated with I135X in a Japanese population in which the prevalence of HLA-B*51:01 and B*52:01 alleles is relatively high (21.9 and 21.1%, respectively). In a Japanese cohort, out of the five

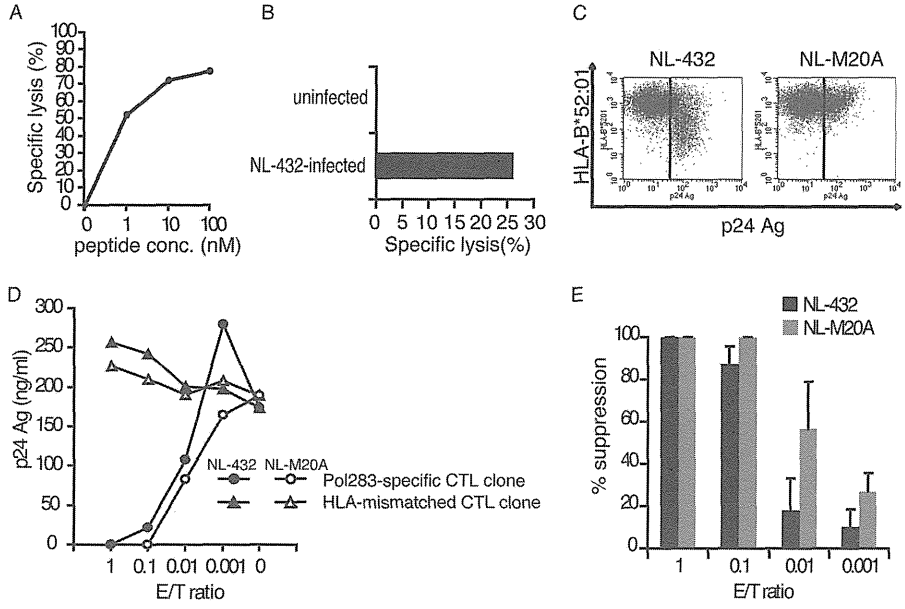

FIG 2 Abilities of HLA-B*52:01-restricted, Pol283-8-specific CD8$^+$ T cell clones to kill HIV-1-infected CD4$^+$ T cells and to suppress HIV-1 replication. (A) Killing activity of an HLA-B*52:01-restricted, Pol283-8-specific CD8$^+$ T cell clone against C1R-B*52:01 cells prepulsed with Pol283-8 peptides. The activity of an HLA-B*52:01-restricted, Pol283-8-specific CD8$^+$ T clone, 1E1, to kill C1R-B*52:01 cells was measured by performing a ^{51}Cr-release assay. (B) Killing activity of HLA-B*52:01-restricted, Pol283-8-specific CD8$^+$ T cell clone 1E1 against CD4$^+$ T cells infected with HIV-1. The ability of the clone to kill CD4$^+$ T cells infected with NL-432 was measured by performing a ^{51}Cr-release assay. (C) Downregulation of HLA-B*52:01 in HIV-1-infected CD4$^+$ T cells. CD4$^+$ T cells derived from an HLA-B*52:01$^+$ donor (HLA-A*11:01/A*24:02, HLA-B*52:01/B*52:01, and HLA-C*12:02/C*14:02) were infected with NL-432 and then cultured for 4 days. The cultured CD4$^+$ T cells were stained with anti-p24 Ag and TÜ109 anti-Bw4 MAbs. (D) Ability of an HLA-B*52:01-restricted, Pol283-8-specific CD8$^+$ T cell clone to suppress the replication of NL-432 and M20A mutant viruses. Suppressing ability was measured at four different E/T cell ratios (1:1, 0.1:1, 0.01:1, and 0.001:1). HIV-1-infected HLA-B*52:01$^+$ CD4$^+$ T cells were cocultured with an HLA-B*52:01-restricted, Pol283-8-specific CTL clone or an HLA-mismatched CTL clone at various E/T cell ratios. HIV-1 p24 Ag levels in the supernatant were measured on day 6 postinfection. (E) Summary of the ability of HLA-B*52:01-restricted, Pol283-8-specific CD8$^+$ T cell clones ($n = 4$) to suppress the replication of Nl-432 and M20A mutant viruses at four different E/T cell ratios.

amino acid mutations that can be generated by a one-nucleotide mutation from Ile, the T mutation was strongly associated with the presence of HLA-B*51:01 ($P = 4.66 \times 10^{-6}$), whereas HLA-B*52:01 was associated not with any single amino acid substitu-

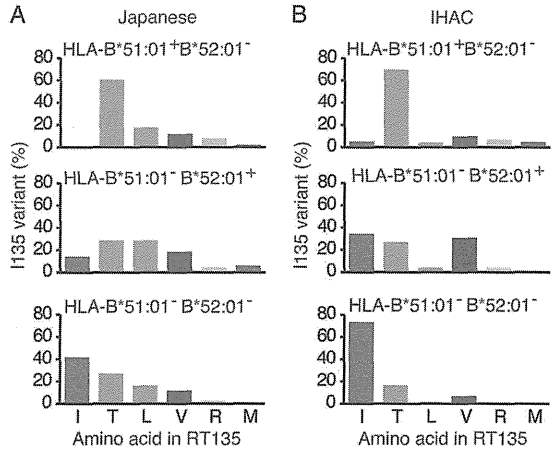

FIG 3 Amino acid variation at RT135 in Japanese individuals. (A) Frequency of the amino acid at RT135 in 51 HLA-B*51:01$^+$ HLA-B*52:01$^-$, 49 HLA-B*51:01$^-$ HLA-B*52:01$^+$, and 151 HLA-B*51:01$^-$ HLA-B*52:01$^-$ Japanese subjects. (B) Frequency of the amino acid at RT135 in 131 HLA-B*51:01$^+$ HLA-B*52:01$^-$, 26 HLA-B*51:01$^-$ HLA-B*52:01$^+$, and 1195 HLA-B*51:01$^-$ HLA-B*52:01$^-$ subjects in three predominantly Caucasian cohorts from Canada, the United States, and Western Australia (IHAC).

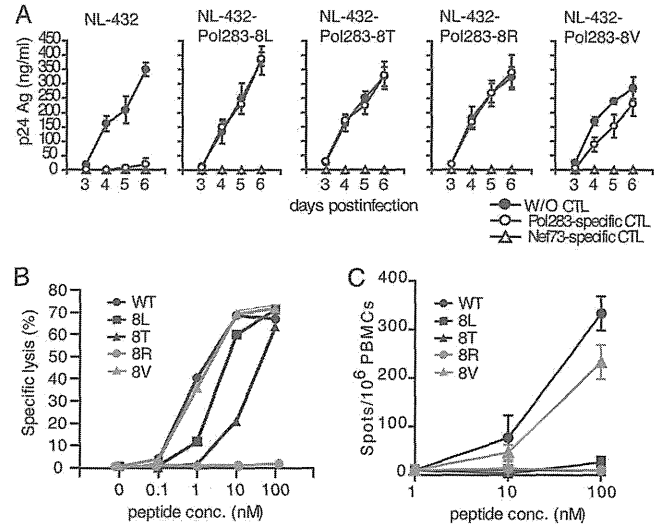

FIG 4 Ability of HLA-B*52:01-restricted, Pol283-8-specific CD8$^+$ T cell clones to suppress the replication of four mutant viruses. (A) Ability of an HLA-B*52:01-restricted, Pol283-8-specific CD8$^+$ T cell clone to suppress the replication of four (8L, 8T, 8R, and 8V) mutant viruses and NL-432. The abilities of an HLA-B*52:01-restricted, Pol283-8-specific CD8$^+$ T cell clone and an HLA-A*1101-restricted Nef73-specific T cell clone to suppress the replication of these viruses were measured at an E/T cell ratio of 1:1 on days 3 to 6. W/O, without. (B) Recognition by an HLA-B*52:01-restricted, Pol283-8-specific CD8$^+$ T cell clone of C1R-B*52:01 cells prepulsed with any one of the four mutant epitope peptides or the wild-type (WT) peptide (8I). (C) Recognition of mutant epitope peptides by *ex vivo* Pol283-8-specific CTLs. The recognition of the Pol283-8 peptide (WT) or the mutant epitope peptide by PBMCs from KI-069 was analyzed by ELISPOT assay.

tion but only with the non-I mutation ($P = 8.77 \times 10^{-4}$, Table 1). The distribution of amino acid variations at RT135 in the HLA-B*51:01$^+$ HLA-B*52:01$^-$ Japanese subjects was different from that in the HLA-B*51:01$^-$ HLA-B*52:01$^+$ ones (Fig. 3). These results suggest that the HLA-B*51:01-restricted CTLs strongly selected the 135T mutation but that the HLA-B*52:01-restricted ones selected a variety of different amino acids at this position in Japanese individuals.

We also analyzed the association of I135X mutations with HLA-B*52:01 and HLA-B*51:01 in three predominantly Caucasian cohorts from Canada, the United States, and Western Australia (International HIV Adaptation Collaborative [IHAC]) (19) comprising >1,200 subjects (Table 1). HLA-B*51:01 was very strongly associated with the I135X mutation (lnOR of 5.71; $P = 1.58 \times 10^{-51}$). Although only 2.1% of the IHAC cohort subjects expressed HLA-B*52:01, this allele was also associated with I135X (lnOR of 3.06; $P = 2.95 \times 10^{-5}$). The T mutation was strongly associated with HLA-B*51:01 ($P = 1.70 \times 10^{-35}$), whereas the T and V mutations were weakly associated with HLA-B*52:01 ($0.0005 < P < 0.005$). Thus, these results showed a similar selection of RT135 mutations by HLA-B*52:01 in the predominantly Caucasian cohort, despite a substantially lower frequency of HLA-B*52:01. The magnitude of the strength of selection by HLA-B*52:01 and HLA-B*51:01 on RT135 did not differ significantly between the two cohorts (Table 1). These results indicate that HLA-B*51:01 strongly selected 135T but that HLA-B*52:01 selected a variety of substitutions at this site (designated I135X) in both the Japanese and non-Japanese cohorts.

Comparison of TCR affinity and abilities of HLA-B*51:01-restricted and HLA-B*52:01-restricted CTLs to suppress HIV-1 replication. We investigated the TCR affinity of HLA-B*51:01-restricted and HLA-B*52:01-restricted CTL clones by using tetramers of the HLA-B*51:01-Pol283 peptide and the HLA-B*52:01-Pol283 peptide complex (HLA-B*51:01 and HLA-B*52:01 tetramers, respectively). The TCR affinity of these CTL clones was compared in terms of EC_{50}. The EC_{50} of the HLA-B*51:01-restricted CTL clones was significantly lower than that of the HLA-B*52:01-restricted CTL clones (Fig. 5A), suggesting that the former CTL clones had TCRs with a higher affinity for the ligand than those of the latter clones. These results imply that the HLA-B*51:01-restricted CTL clones could recognize the HIV-1-infected targets more effectively than HLA-B*52:01-restricted ones.

Since CD4$^+$ T cells derived from an HLA-B*52:01 homozygous individual were used in the experiment shown in Fig. 2D and E, the ability of the HLA-B*52:01-restricted CTL clones to suppress the replication of NL-432 may have been overestimated. To evaluate and compare the abilities of HLA-B*51:01-restricted and HLA-B*52:01-restricted CTL clones to suppress the replication of NL-432, we used CD4$^+$ T cells from individuals expressing HLA-B*51:01$^+$/B*52:01$^-$, HLA-B*51:01$^-$/B*52:01$^+$, or HLA-B*51:01$^+$/B*52:01$^+$ (Fig. 5B). Two HLA-B*51:01-restricted CTL clones strongly inhibited the replication of HIV-1 in cultures of NL-432-infected HLA-B*51:01$^+$/B*52:01$^-$ CD4$^+$ T cells but not in those of HLA-B*51:01$^-$/B*52:01$^+$ cells, whereas two HLA-B*52:01-restricted CTL clones strongly inhibited the replication of HIV-1 in cultures of NL-432-infected HLA-B*51:01$^-$/B*52:01$^+$ CD4$^+$ T cells but not in those of HLA-B*51:01$^+$/B*52:01$^-$ cells (Fig. 5B, left and middle). The ability of the HLA-B*51:01-restricted CTL clones to suppress the replication of HIV-1 was greater than that of the HLA-B*52:01-restricted CTL clones. This was confirmed by the experiment with HLA-B*51:01$^+$/B*52:01$^+$ CD4$^+$ T cells (Fig. 5B, right). Although both HLA-B*51:01-restricted and HLA-B*52:01-restricted CTL clones strongly inhibited the replication of HIV-1 in the cultures of NL-432-infected HLA-B*51:01$^+$/B*52:01$^+$ CD4$^+$ T cells, the former clones exhibited a greater ability to suppress the replication of HIV-1 than did the latter cells. These results indicate that the HLA-B*51:01-restricted CTL clones had a stronger ability to suppress HIV-1 replication than the HLA-B*52:01-restricted clones. Taken together, both our *in vitro* and our *in vivo* (population level HLA-association) data suggest that immune pressure on RT135 by HLA-B*51:01-restricted T cells was stronger than that imposed by HLA-B*52:01-restricted cells.

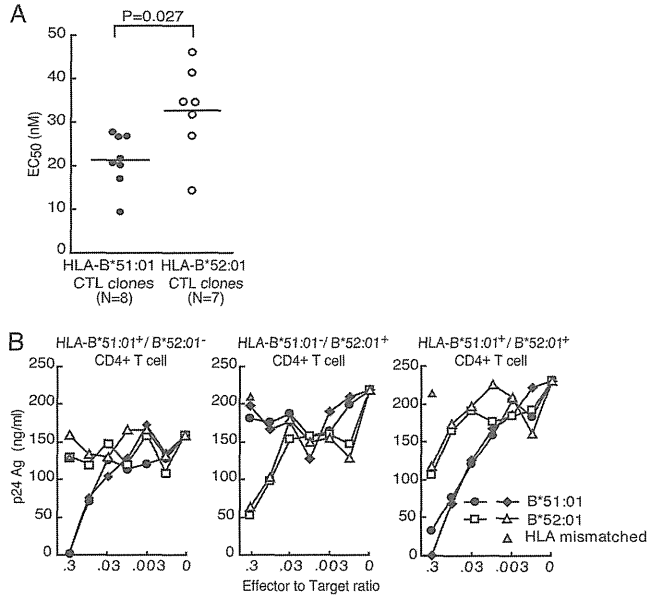

FIG 5 Differences between HLA-B*51:01-restricted and HLA-B*52:01-restricted CD8$^+$ T cell clones in TCR avidity and the ability to suppress HIV-1 replication. (A) TCR avidity of the HLA-B*51:01-restricted and HLA-B*52:01-restricted CTL clones expressed as EC_{50}. The ability of the TCRs of HLA-B*51:01-restricted and HLA-B*52:01-restricted CTL clones to bind HLA-B*51:01 tetramers and HLA-B*52:01 tetramers, respectively, was measured in terms of the MFI of each CTL clone stained with the tetramers at concentrations of 5 to 1,000 nM. (B) The ability of two HLA-B*51:01-restricted and two HLA-B*52:01-restricted CD8$^+$ T cell clones to suppress HIV-1 was measured at six different E/T cell ratios (0.3:1, 0.1:1, 0.03:1, 0.01:1, 0.003:1, and 0.001:1). CD4$^+$ T cells from individuals expressing HLA-B*51:01$^+$/B*52:01$^-$, HLA-B*51:01$^-$/B*52:01$^+$, or HLA-B*51:01$^+$/B*52:01$^+$ were infected with NL-432 and then cocultured with a given Pol283-8-specific CTL clone or an HLA-mismatched CTL clone. HIV-1 p24 Ag levels in the supernatant were measured on day 5 postinfection.

Structural basis of the difference in recognition between HLA-B*52:01- and HLA-B*51:01-restricted CTLs. In order to investigate the structural basis of the difference in recognition between HLA-B*52:01- and HLA-B*51:01-restricted CTLs, we performed a crystallographic study of the HLA-B*52:01 molecule complexed with the Pol283-8 peptide. The recombinant HLA-B*52:01 protein was crystallized, and by using the molecular replacement method, the three-dimensional structure of HLA-B*52:01 complexed with the Pol283-8 peptide was successfully determined. The crystal and statistical data are summarized in Table S1 in the supplemental material. The overall structure and peptide-binding mode were similar to those of HLA-B*51:01 complexed with the same Pol283-8 peptide (Fig. 6A and B), which

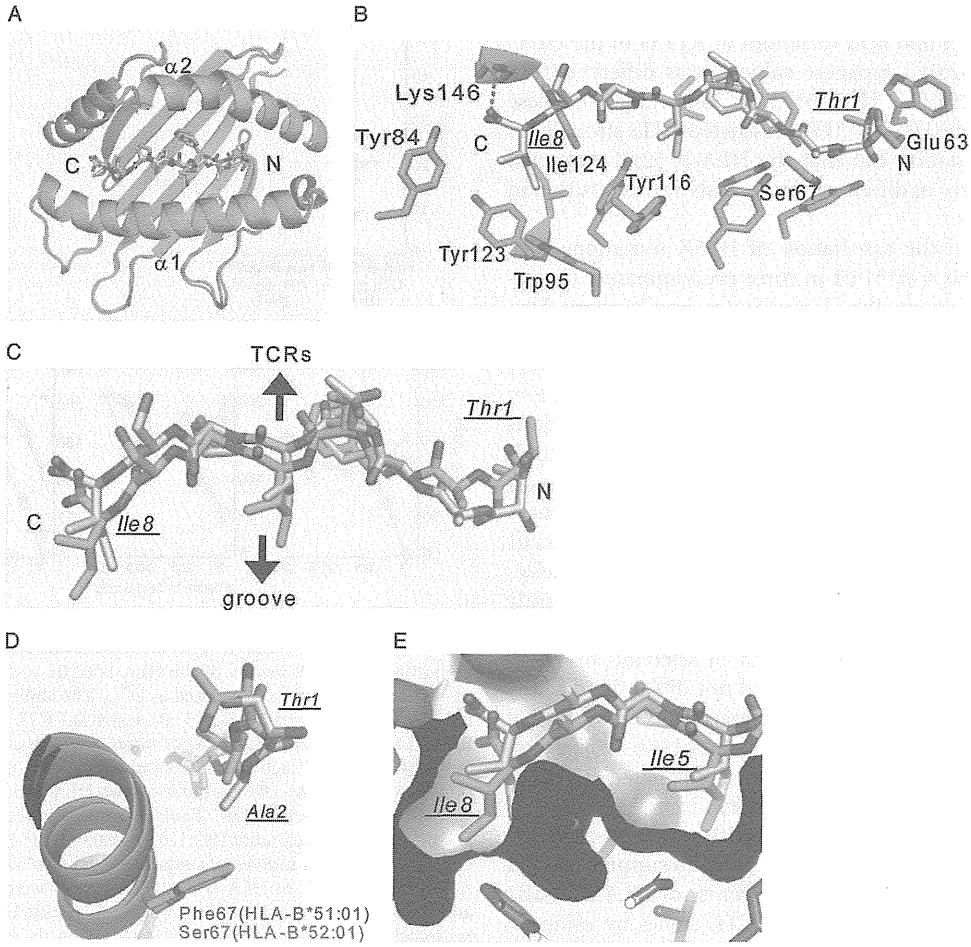

FIG 6 Structural comparison of HLA-B*52:01 and HLA-B*51:01 molecules complexed with the Pol283-8 peptide. (A) Crystal structures of HLA α1-α2 domains complexed with the Pol283-8 peptide (stick model) on the HLA-B*52:01 (green, yellow) and HLA-B*51:01 (cyan, cyan) complexes. This same coloring also applies to panels B to E. (B) Pol283-8 peptide and interacting side chains on the HLA-B*52:01 complex. Hydrogen bonds are shown as blue dotted lines. (C) Comparison of the Pol283-8 peptide conformations of HLA-B*52:01 and HLA-B*51:01 complexes. (D) N-terminal side of HLA-B*52:01 and HLA-B*51:01 complexes. (E) C-terminal side of HLA-B*52:01 and HLA-B*51:01 complexes. Surface presentation for the α1-α2 domains is shown in gray.

we had previously reported (45). This finding explains the cross presentation of this peptide by both HLA alleles. On the other hand, there was a notable conformational difference in the N-terminal region of the peptide between the two alleles (Fig. 6C and D). The replacement of Phe67 of HLA-B*51:01 with Ser in HLA-B*52:01 makes a local space, causing the N-terminal region of the peptide (T1 and A2) to reside deeper in the peptide-binding groove. Furthermore, the Gln63Glu mutation in HLA-B*52:01 affords a new interaction with the T1 residue of the peptide. These changes would, to some extent, have hidden the side chains of T1 and A2 (flat surface) from the TCRs, which may have reduced their interactions with TCRs on the HLA-B*52:01-restricted CTLs. On the other hand, the conformation of the C-terminal region of the peptide complexed with HLA-B*51:01 or HLA-B*52:01 was similar, even though C-terminal Ile8 of the peptide exhibited shallower penetration of the hydrophobic groove in the case of HLA-B*52:01 than in that of HLA-B*51:01 (Fig. 6C and E). These results may indicate that the relatively flat surface of the N-terminal side of the peptide contributed to the lower affinity for TCRs in the case of HLA-B*52:01.

DISCUSSION

HLA-B*52:01 and HLA-B*51:01 differ by only two residues, at positions 63 and 67 (44). Substitutions at these residues affect the formation of the B pocket in the peptide-binding pocket (45), suggesting the possibility that HLA-B*52:01 has a peptide motif different from that of HLA-B*51:01. Indeed, HLA-B*52:01-binding peptides have P2 primary anchors that are different from HLA-B*51:01-binding ones (30, 46). Since the Pol283-8 epitope carries Ala at its second position and Ile at the C terminus of the peptide, it is likely that this peptide would effectively bind to HLA-B*51:01 but not to HLA-B*52:01. However, the results of the HLA stabilization assay demonstrated that the Pol283-8 peptide did effectively bind to HLA-B*52:01. Since the HLA-B*52:01-binding peptide is known to have Pro as its preferred P2 anchor residue, this peptide carrying Ala at position 2 may be capable of binding to HLA-B*52:01. A previous study showed cross-recognition of alloreactive T cells between HLA-B*51:01 and HLA-B*52:01 (47, 48), indicating that some self-peptides can be presented by both of these HLA class I molecules. The findings on the crystal structure